

---

# Accelerated Diffusion Models via Speculative Sampling

---

Valentin De Bortoli<sup>\*1</sup> Alexandre Galashov<sup>\*1</sup> Arthur Gretton<sup>1</sup> Arnaud Doucet<sup>1</sup>

## Abstract

Speculative sampling is a popular technique for accelerating inference in Large Language Models by generating candidate tokens using a fast draft model and accepting or rejecting them based on the target model’s distribution. While speculative sampling was previously limited to discrete sequences, we extend it to diffusion models, which generate samples via continuous, vector-valued Markov chains. In this context, the target model is a high-quality but computationally expensive diffusion model. We propose various drafting strategies, including a simple and effective approach that does not require training a draft model and is applicable out of the box to any diffusion model. Our experiments demonstrate significant generation speedup on various diffusion models, halving the number of function evaluations, while generating exact samples from the target model.

## 1. Motivation

Denosing diffusion models (DDMs), introduced by Sohl-Dickstein et al. (2015) and further developed by Ho et al. (2020) and Song et al. (2021), are generative models exhibiting state-of-the-art performance in a wide variety of domains. The core concept behind DDMs is the progressive transformation of a data distribution into a Gaussian distribution through the addition of noise. Sample generation is achieved by simulating an approximation of the time-reversal of this noising process. This requires multiple evaluations of a neural network that approximates the scores of the noising process, and typically involves simulating a Markov chain over hundreds of steps.

Since sample generation is computationally expensive, several techniques have been proposed to accelerate it. These include distillation techniques (e.g. Salimans & Ho, 2022; Meng et al., 2023; Song et al., 2023), better sampling schemes (e.g. Karras et al., 2022; Lu et al., 2022; Zhang & Chen, 2023) and parallel simulation methods (e.g. Shih

et al., 2023; Chen et al., 2024). However, distillation techniques inherently require training a student model and often underperform compared to the teacher model (Dieleman, 2024). While better sampling schemes can improve performance, using too small a number of steps does degrade performance, see for instance (Karras et al., 2022). Finally, parallel simulation methods relying on Picard iterations over a sliding window have been proposed (Shih et al., 2023; Chen et al., 2024; Tang et al., 2024). However, they require iterating the parallel sampling procedure on a window until errors fall below some pre-specified tolerance.

In the context of Large Language Models (LLMs), various techniques have also been proposed to speed up inference, which we briefly review in Section 2. Notably, *speculative sampling*, first introduced by Leviathan et al. (2023) and later proposed independently by Chen et al. (2023), has become prominent in this area and has spawned numerous extensions (Xia et al., 2024). Given a target LLM, this algorithm enables faster sampling than serial token decoding without compromising quality, as the sampled tokens remain exactly distributed according to the target model’s distribution. This is achieved by considering a smaller and faster LLM model generating a draft sequence. The target model is then used to compute *in parallel* the conditional probabilities of these draft tokens, and these probabilities are used to decide sequentially whether to accept or reject the draft tokens. Upon the first rejection, a new token is sampled using an adjusted distribution combining the draft and target distributions. Many extensions of speculative sampling have been proposed to reduce latency; see Xia et al. (2024) and further related works in Section 5.

In the present work, we adapt speculative sampling to accelerate DDMs. We assume a computationally cheap draft model that generates a sequence of draft states for the denoising Markov chain of a target DDM. The transition probability densities of these states under the target model are then computed *in parallel* and used to sequentially accept/reject the draft states. At rejection, a new state is sampled from an adjusted distribution dependent on both the draft and target distributions; see Figure 1. As for LLMs, the procedure is designed such that it outputs samples distributed exactly according to the target DDM.

Wang et al. (2024) concurrently proposed an adaptation of

<sup>\*</sup>Equal contribution <sup>1</sup>Google DeepMind. Correspondence to: Valentin De Bortoli <vdebortoli@google.com>.

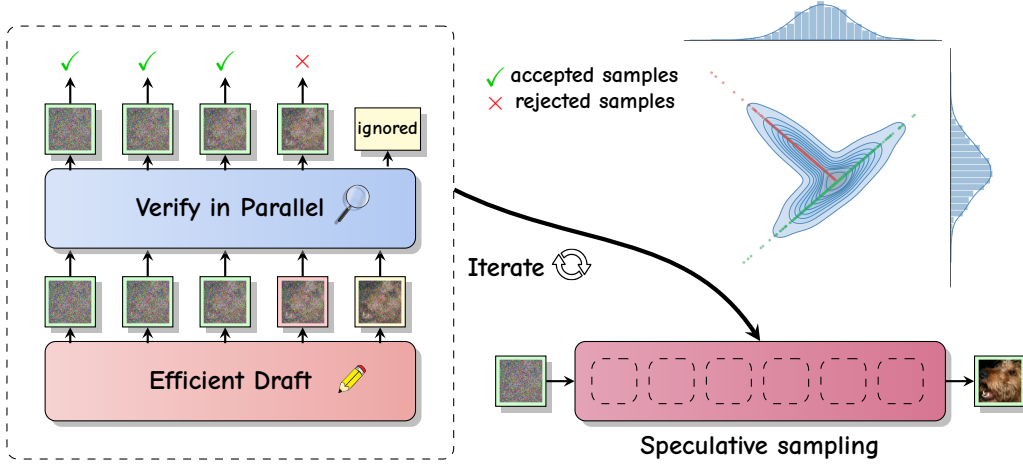


Figure 1. Overview of Speculative Sampling for accelerated simulation of diffusion models.

the speculative sampling procedure for continuous-valued autoregressive processes, specifically for Masked Autoregressive models (Li et al., 2024b). In this continuous state-space context, they sample from the adjusted distribution appearing at rejection using a standard rejection sampling algorithm. However, as we demonstrate in Section 3.2, this approach is, on average, more computationally expensive than directly sampling from the target model in our context. Furthermore, it exhibits counter-intuitive performance degradation as the draft model more closely approximates the target model. We present a method to circumvent these issues while retaining the optimality properties of speculative sampling. Our contributions are summarized below. All the proofs are given in the Supplementary Material.

- We investigate several drafting strategies (Section 3.1 and Appendix B). As with LLMs, one can rely on a “cheap” diffusion model as draft model, or use a draft model learned from the target model. However these approaches require significant overheads. We propose here a simple and effective approach that proposes a draft model relying solely on the target model. This eliminates any need for learning a separate draft model, and is applicable to any diffusion model.
- By leveraging the connections between speculative sampling and coupling techniques (Lindvall, 1992), first observed by Sun et al. (2023) in the context of LLMs, we show in Section 3.3 that we can sample efficiently from a novel adjusted distribution for DDMs using reflection maximal coupling (Bou-Rabee et al., 2020). Our procedure returns exact samples from the target model, and it is optimal in the sense that it maximizes the probability of accepting each draft state.
- In Section 4, we present complexity analysis and a lower bound on the acceptance ratio.

- The proposed method achieves significant speed-ups for image generation on CIFAR10, and LSUN using pixel space diffusion models, without any loss of quality (Section 6). Furthermore, we show similar speed-ups in robotics for policy generation.

## 2. Speculative Sampling for LLMs

We begin with a review of speculative sampling for LLMs. Consider two probability distributions  $q$  and  $p$  for sequences on some finite space  $\mathcal{X}$ . In this context  $q$  corresponds to the joint distribution of tokens for the target LLM, while  $p$  represents the draft model.

### 2.1. Speculative Sampling for Autoregressive Targets

---

#### Algorithm 1 Speculative Sampling for LLM

---

**Require:** Lookahead integer  $L$ , maximum length  $K$ , draft model  $p$ , target model  $q$ , initial context  $X_0, \dots, X_{n_0}$ .

Set  $n \leftarrow n_0$

**while**  $n < n_0 + K$  **do**

Sample  $\tilde{X}_{n+1:n+L} \sim p(\cdot | X_{0:n})$

Get  $p_{n+j} = p(\cdot | X_{0:n}, \tilde{X}_{n+1:n+j-1}), j \in [L]$ .

Get  $q_{n+j} = q(\cdot | X_{0:n}, \tilde{X}_{n+1:n+j-1}), j \in [L]$ .

**for**  $k = n + 1 : n + L$  **do**

$(\tilde{X}_k, X_k, \text{bool}) \leftarrow \text{REJECTION}(p_k, q_k, \tilde{X}_k)$

**if** not(bool) or  $X_k = \text{EOS}$  **then**

Exit For Loop

**end if**

**end for**

Set  $n \leftarrow k$

**end while**

**return**  $X_{n_0+1:n}$

---

Speculative sampling generates  $L$  candidate tokens accord-

ing to the draft model  $p$  which are scored in parallel using the target model  $q$ . They are then accepted sequentially using an adjusted rejection sampling algorithm. At the first rejection, one needs to sample a new token from an adjusted distribution denoted  $r$ . A new set of  $L$  candidate tokens is then generated, and so on. This is detailed in Algorithm 1 using notation  $z_{k:\ell} = (z_k, z_{k+1}, \dots, z_\ell)$  for  $k \leq \ell$  and  $z_{k:\ell} = \emptyset$  for  $k > \ell$  for any sequence  $(z_k)_{k \in \mathbb{N}}$  and  $[k] = \{1, \dots, k\}$  for any positive integer  $k$ . The rejection mechanism is described in Algorithm 2.

---

**Algorithm 2** REJECTION ( $p, q, X$ )
 

---

**Require:** Proba. distributions  $p, q$  and  $X \sim p$ .

Sample  $U \sim \text{Unif}[0, 1]$ .

`bool` =  $\mathbb{I}[U \leq \min(1, q(X)/p(X))]$ .

**if** `bool` **then**

    Set  $Y = X$ .

**else**

$Y \sim r(\cdot)$ ,  $r(x) \propto \max(0, q(x) - p(x))$ .

**end if**

**return**  $(X, Y, \text{bool})$  where  $Y \sim q$ .

---

In (Chen et al., 2023; Leviathan et al., 2023), the draft sequence is sampled using a ‘‘cheap’’ autoregressive LLM, i.e.,  $\tilde{X}_{n+1} \sim p(\cdot | X_{0:n})$ ,  $\tilde{X}_{n+2} \sim p(\cdot | X_{0:n}, \tilde{X}_{n+1})$ , ...,  $\tilde{X}_{n+L} \sim p(\cdot | X_{0:n}, \tilde{X}_{n+1:n+L-1})$ . However, this does not have to be the case, and any distribution  $p(x_{n+1:n+L} | x_{0:n})$  can be used<sup>1</sup>, e.g., in Medusa (Cai et al., 2024) one samples the draft tokens in parallel by considering a factorized draft distribution  $p(x_{n+1:n+L} | x_{0:n}) = \prod_{k=n+1}^{n+L} p(x_k | x_{0:n})$ .

## 2.2. Adjusted Rejection Sampling as Maximal Coupling

At the core of speculative sampling lies an adjusted rejection sampling mechanism which allows for sampling from the (conditional) distribution of a token  $q(x) := q(x | \text{past tokens})$  for a target LMM given the (conditional) distribution  $p(x) := p(x | \text{past tokens})$  of a token for a draft model.

As pointed out by Sun et al. (2023), this procedure, summarized in Algorithm 2, is well-known in the probability literature, and the joint distribution of  $(X, Y)$  it induces is a so-called maximal coupling; see e.g. (Lindvall, 1992), Section 4.5 in (Thorisson, 2000) and (Jacob, 2021) for a comprehensive introduction. Maximal couplings denote any distribution on  $(X, Y)$  maximizing the probability that  $X = Y$  while  $X \sim p$  and  $Y \sim q$ . For completeness, without any claim for originality, see Proposition 2.1 for

<sup>1</sup>In this context, the distributions  $\{p(x_{n+1:n+L} | x_{0:n})\}_{n \geq n_0}$  are not usually compatible, i.e., they are not the conditional distributions of a joint distribution. To be more precise, we should write  $p_n(x_{n+1:n+L} | x_{0:n})$  instead of  $p(x_{n+1:n+L} | x_{0:n})$  but we slightly abuse notation here.

a formal statement and the supplementary material for a proof. Contrary to standard rejection sampling, this does not require having to upper bound  $q(x)/p(x)$  and admits a bounded and short running time.

**Proposition 2.1:** *Algorithm 2 outputs samples  $(X, Y)$  such that marginally one has  $X \sim p$  and  $Y \sim q$ . It is optimal in the sense that it is a procedure that maximizes the probability that  $X = Y$  under the constraints  $X \sim p$ ,  $Y \sim q$ . Additionally, we have*

$$\mathbb{P}(X \neq Y) = \|p - q\|_{\text{TV}},$$

where  $\|p - q\|_{\text{TV}} := \frac{1}{2} \sum_{x \in \mathcal{X}} |p(x) - q(x)|$ .

## 3. Speculative Sampling for Diffusion Models

We now present our main contribution, which is the adaptation of speculative sampling to DDMs. Our DDM target model and some drafting strategies are given in Section 3.1, leading to our speculative sampling procedure in Algorithm 3. As for LLMs, this algorithm requires an adjusted rejection sampling procedure. After analyzing the difficulties of an implementation of Algorithm 2 in the context of DDMs (Section 3.2), an original solution resolving these difficulties is presented in Section 3.3.

### 3.1. Denoising diffusion models, draft models and speculative sampling

We first define the target DDM model we want to sample from. Following Song et al. (2021), consider a *forward* noising process where  $\mathbf{X}_0 \sim q_{\text{data}}$  and  $d\mathbf{X}_t = f_t \mathbf{X}_t dt + g_t d\mathbf{B}_t$ , where  $(\mathbf{B}_t)_{t \in [0,1]}$  is a  $d$ -dimensional Brownian motion. Let  $q_t$  the density of  $\mathbf{X}_t$ , we select  $f_t, g_t$  such that  $q_1 \approx \mathcal{N}(0, \text{Id})$ . We then consider the process  $(\mathbf{Y}_t)_{t \in [0,1]}$  with  $\mathbf{Y}_0 \sim q_1$  and

$$d\mathbf{Y}_t = b_t(\mathbf{Y}_t) + \varepsilon g_{1-t} d\mathbf{W}_t, \quad (1)$$

for  $b_t(x) = -f_{1-t}x + \frac{1+\varepsilon^2}{2}g_{1-t}^2s_{1-t}(x)$  where  $s_t(x) = \nabla \log q_t(x)$  is the *Stein score*,  $(\mathbf{W}_t)_{t \in [0,1]}$  is another Brownian motion and  $\varepsilon \geq 0$  is an hyperparameter which controls the stochasticity level of  $(\mathbf{Y}_t)_{t \in [0,1]}$  (Albergo et al., 2023), referred to as the *churn* parameter in the literature (Karras et al., 2022). This process is such that  $\mathbf{Y}_{1-t} \sim q_t$  for all  $t \in [0, 1]$  and corresponds to the *time-reversal* of  $(\mathbf{X}_t)_{t \in [0,1]}$  for  $\varepsilon = 1$ . In practice,  $b_t$  is approximated using a neural network denoted  $b_t^q$ . At inference we consider  $K + 1$  discretization steps and let  $\gamma = 1/K$  and  $(t_k)_{k=0}^K$  with  $t_k = k\gamma$ ; the corresponding distribution of the resulting Markov chain obtained by the Euler–Maruyama discretisation of (1) and initialized at  $\mathcal{N}(0, \text{Id}) \approx q_1$  is denoted  $q(y_{0:K}) = q(y_0) \prod_{k=1}^K q(y_k | y_{k-1})$  where

$$q(y_k | y_{k-1}) = \mathcal{N}(y_k; m_{k-1}^q(y_{k-1}), \sigma_{k-1}^2 \text{Id}), \quad (2)$$

with  $q(y_0) = \mathcal{N}(y_0; 0, \text{Id}) \approx q_1(y_0)$ ,  $m_k^q(y_k) = y_k + \gamma b_{t_k}^q(y_k)$  and  $\sigma_k = \sqrt{\gamma \varepsilon g_{1-t_k}}$ . The distribution (2) defines the target model in our speculative sampling procedure.

Speculative sampling requires specifying a draft model. All the draft models we consider are of the form  $p(y_{n+1:n_L}|y_n) = \prod_{k=n+1}^{n_L} p(y_k|y_{n:k-1})$  where  $n_L = \min(n+L, K)$ ,  $L$  is the length of the draft sequence and

$$p(y_k|y_{n:k-1}) = \mathcal{N}(y_k; m_{k-1}^p(y_{n:k-1}), \sigma_{k-1}^2 \text{Id}). \quad (3)$$

**Independent draft model.** A first choice, similar to the original speculative sampling algorithm (Leviathan et al., 2023), is to consider a draft model with the same sampling strategy as  $q$  but with an approximation  $b_t^p$  which is cheaper to evaluate than  $b_t^q$ . Hence, the draft model satisfies  $p(y_k|y_{n:k-1}) = p(y_k|y_{k-1})$  with

$$m_k^p(y_{n:k}) = y_k + \gamma b_{t_k}^p(y_k), \quad \sigma_k = \sqrt{\gamma \varepsilon g_{1-t_k}}. \quad (4)$$

This choice of draft requires the availability of a cheaper DDM. For  $p$  and  $q$  to be close and to obtain better performance (i.e., higher acceptance rate of the draft states), this requires training  $p$  on the same dataset as  $q$ , which would be costly and might not be feasible. In addition even if  $p$  and  $q$  are trained with the same architecture on the same dataset, there could still be a significant mismatch between  $b^p$  and  $b^q$ . This is because, depending on the seed, diffusion models can learn different mappings from the Gaussian distribution to the data distribution.

**Frozen target draft model.** Another popular choice in speculative sampling is to derive a draft model directly from the target model, see for instance (Cai et al., 2024). In the context of diffusion models, we consider here a very simple draft model where  $p(y_k|y_{n:k-1}) = p(y_k|y_n, y_{k-1})$  with

$$m_k^p(y_{n:k}) = y_k + \gamma b_{t_n}^q(y_n), \quad \sigma_k = \sqrt{\gamma \varepsilon g_{1-t_k}}. \quad (5)$$

This draft model is similar to the target model, except that we replace  $b_{t_k}^q(y_k)$  by  $b_{t_n}^q(y_n)$ . Importantly, on a window of size  $L$ , we only need to query the target model *once* in order to draw a draft sequence. This strategy is thus computationally inexpensive, requires no additional training and allows parallel sampling of the draft sequence. However, the differences between the draft and target models can be large near the data distribution as the score function typically exhibits significant variation. Consequently,  $b_{t_n}^q(y_n)$  may deviate substantially from  $b_{t_k}^q(y_k)$  when  $k, n, K$  are close, rendering the approximation  $b_{t_k}^q(y_k) \approx b_{t_n}^q(y_n)$  inaccurate.<sup>2</sup> This issue can be addressed at higher computational cost using alternative and more involved drafting procedures, as discussed in Appendix B.

<sup>2</sup>More sophisticated approximations, such as local linearization (Shoji & Ozaki, 1998), could improve accuracy but their computational cost is prohibitive in high dimension.

---

### Algorithm 3 Speculative Sampling for DDM

---

**Require:** Lookahead integer  $L$ , sequence length  $K$ , target model  $q$  and draft model  $p$ .

Sample  $Y_0 \sim \mathcal{N}(0, \text{Id})$  and set  $n = 0$ .

**while**  $n < K$  **do**

Set  $\tilde{Y}_n \leftarrow Y_n$  and  $n_L \leftarrow \min(n+L, K)$

Sample draft states  $\tilde{Y}_{n+1:n_L} \sim p(\cdot|Y_n)$  using (3).

Get means of  $p_{n+j} = p(\cdot|Y_{n:n+j-1})$ ,  $j \in [n_L - n]$

Get means of  $q_{n+j} = q(\cdot|\tilde{Y}_{n+j-1})$ ,  $j \in [n_L - n]$

**for**  $k = n+1 : n_L$  **do**

$(\tilde{Y}_k, Y_k, \text{bool}) \leftarrow \text{REJECTION}(p_k, q_k, \tilde{Y}_k)$ .

**if** **not**(bool) **then**

Exit For Loop

**end if**

**end for**

Set  $n \leftarrow k$ .

**end while**

**return**  $Y_{0:K}$

---

Having now defined the target and draft model, we present Algorithm 3, our speculative sampling algorithm for diffusion models. This algorithm is similar in principle to Algorithm 1 for LLMs. Note that the rejection steps within the for loop are also implemented in parallel. However, the REJECTION step in our algorithm requires a substantially different implementation compared to the one defined by Algorithm 2 used for LLMs. This difference arises because directly applying the rejection mechanism of Algorithm 2 to diffusion models presents significant challenges, as we will demonstrate.

### 3.2. Adjusted Rejection Sampling: Implementation Issues

Using Algorithm 2 to define REJECTION in Algorithm 3 would yield a valid speculative sampling algorithm for diffusion models, i.e., this algorithm would produce a Markov chain exactly distributed according to the target model,  $Y_{0:K} \sim q$ , and Proposition 2.1 would also apply directly.<sup>3</sup> However, we show below that implementing Algorithm 2 is problematic in the context of diffusion models. If a draft state is rejected at iteration  $k$ , where  $k > n$ , we must then sample  $Y_k$  from

$$r(x) = \frac{\max(0, q(x) - p(x))}{\int_{\mathbb{R}^d} \max(0, q(x) - p(x)) dx}, \quad (6)$$

for  $q(y_k) := q(y_k|y_{k-1})$ ,  $p(y_k) := p(y_k|y_{n:k-1})$ . Although straightforward for LLMs due to the discrete nature of  $r(x)$ , a satisfactory solution for continuous state-spaces

<sup>3</sup>The proof of Proposition 2.1 recalled in Appendix A extends straightforwardly from  $\mathcal{X}$  finite to  $\mathbb{R}^d$



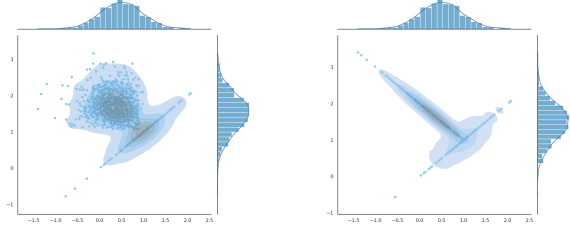


Figure 2. Two distinct maximal couplings between  $p = \mathcal{N}(0.5, 0.25)$  and  $q = \mathcal{N}(1.5, 0.25)$ . On the left the maximal coupling given by Algorithm 2 and on the right the reflection maximal coupling given by Algorithm 4. Both are such that  $X \sim p$  and  $Y \sim q$  marginally and have the exact same probability that  $X = Y$ .

remains elusive. Leveraging the fact that

$$r(x) \propto q(x)(1 - \min(1, p(x)/q(x))), \quad (7)$$

we could sample from  $r(x)$  using standard rejection sampling. Using  $q(x)$  as proposal, the acceptance probability is  $1 - \min(1, p(x)/q(x))$  so that the average acceptance probability is

$$\int q(x)(1 - \min(1, p(x)/q(x)))dx = \|p - q\|_{\text{TV}}.$$

This is an approach analyzed by Jacob (2021) and adopted by Wang et al. (2024) for continuous-valued autoregressive processes. From standard results on rejection sampling, it is known that the number of trials to simulate from the target  $q$  before acceptance follows a geometric distribution with parameter  $\|p - q\|_{\text{TV}}$ . This distribution has mean  $1/\|p - q\|_{\text{TV}}$  and variance  $(1 - \|p - q\|_{\text{TV}})/\|p - q\|_{\text{TV}}^2$  (see (Jacob, 2021) for instance). This implementation of Algorithm 2 proves inefficient, as demonstrated by the following simple analysis. With probability  $\|p - q\|_{\text{TV}}$ , one needs to sample from (7) and, due to the properties of the geometric distribution, the expected number of samples from  $q$  we need is  $\|p - q\|_{\text{TV}} \times (1/\|p - q\|_{\text{TV}}) = 1$ . This rejection sampling procedure is thus practically useless, as it requires sampling on average from both  $p$  and  $q$ , as well as computing the acceptance probability  $\min(1, q(x)/p(x))$ . Another undesirable property of this implementation is that the variance of the number of samples from  $q$  one would have to simulate increases rapidly as the draft model  $p$  better approximates the target  $q$  (i.e., as  $\|p - q\|_{\text{TV}}$  decreases). These issues have been extensively reported in the literature (Jacob, 2021).

### 3.3. Adjusted Rejection Sampling via Reflection-Maximal Coupling

As discussed in Section 2.2, the adjusted rejection sampling procedure from Algorithm 2 is identical to a specific maximal coupling described, for example, in (Lindvall, 1992). For DDMs, we have shown that implement-

ing this procedure is challenging. However, it is essential to note that maximal couplings are *not* unique. Bou-Rabee et al. (2020) proposed an algorithm known as *reflection maximal coupling* to implement a maximal coupling for two Gaussian distributions  $\mathcal{N}(m^p, \sigma^2 \text{Id})$  and  $\mathcal{N}(m^q, \sigma^2 \text{Id})$ . This is directly applicable to diffusions models, since  $p(y_k | y_{n:k-1}) = \mathcal{N}(y_k; m_{k-1}^p(y_{n:k-1}), \sigma_{k-1}^2 \text{Id})$  and  $q(y_k | y_{k-1}) = \mathcal{N}(y_k; m_{k-1}^q(y_{k-1}), \sigma_{k-1}^2 \text{Id})$  are Gaussian distributions with different means but identical variances. Introduced to establish convergence results for Hamiltonian Monte Carlo, this procedure is noteworthy for its conciseness and its bounded and short running time. We detail it in Algorithm 4.

Direct calculations show that the acceptance probability of  $X \sim \mathcal{N}(m^p, \sigma^2 \text{Id})$  computed with this procedure is identical to the one used in Algorithm 2. This follows from the fact that  $q(X)/p(X) = \mathcal{N}(Z + \Delta; 0, \text{Id})/\mathcal{N}(Z; 0, \text{Id})$  with  $\Delta = (m^p - m^q)/\sigma$  for  $X = m^p + \sigma Z$ . At acceptance, we also have  $Y = X$  as in Algorithm 2. However, Algorithm 4 differs fundamentally from Algorithm 2, as upon rejection of the draft state, the new state is computed *deterministically* as a function of the rejected state, instead of sampling from (6); see Figure 2 for an illustration. This requires only one evaluation of the target  $q(y_k | y_{k-1})$  to obtain the state  $Y_k$ . Therefore, we use Algorithm 4 for REJECTION in our implementation of speculative sampling. A detailed full implementation is provided in Algorithm 5. The following proposition, which parallels Proposition 2.2, establishes the correctness of the method and follows Section 2.3.2 from Bou-Rabee et al. (2020).

**Proposition 3.1 (Reflection Coupling):** *Algorithm 4 outputs samples  $(X, Y)$  such that marginally  $X \sim p$  and  $Y \sim q$  where  $p(x) = \mathcal{N}(x; m^p, \sigma^2 \text{Id})$  and  $q(x) = \mathcal{N}(x; m^q, \sigma^2 \text{Id})$ . Additionally, it maximizes the probability that  $X = Y$  and*

$$\mathbb{P}(X \neq Y) = \|p - q\|_{\text{TV}} = 2\Phi(\sigma^{-1}\|m^p - m^q\|/2) - 1,$$

where  $\|p - q\|_{\text{TV}} = \frac{1}{2} \int |p(x) - q(x)|dx$  and  $\Phi$  is the c.d.f. of the standard normal random variable.

This result shows that the efficiency of speculative sampling at time  $k$  - i.e., the probability of accepting a draft state - is a decreasing function of  $\|m_{k-1}^p(\tilde{Y}_{n:k-1}) - m_{k-1}^q(\tilde{Y}_{k-1})\|/\sigma_{k-1}$ . This means that, as expected, a draft model must reasonably approximate the target for good performance.

## 4. Theoretical analysis

We provide an analysis of the proposed methodology. We derive an approximation of the complexity of speculative sampling in Section 4.1, and a lower-bound on the accep-

**Algorithm 4** REJECTION ( $p, q, X$ ) for two Gaussians with same covariance

**Require:** Gaussians  $p(x) = \mathcal{N}(x; m^p, \sigma^2 \text{Id}), q(x) = \mathcal{N}(x; m^q, \sigma^2 \text{Id})$  and  $X \sim p$ .  
 Set  $\Delta = (m^p - m^q)/\sigma$  and  $e = \Delta/\|\Delta\|$ .  
 Let  $Z = (X - m^p)/\sigma$ .  
 Sample  $U \sim \text{Unif}[0, 1]$ .  
 $\text{bool} = \mathbb{I}\left[U \leq \min\left(1, \frac{\mathcal{N}(Z+\Delta; 0, \text{Id})}{\mathcal{N}(Z; 0, \text{Id})}\right)\right]$ .  
**if** bool **then**  
     Set  $Y = X$ .  
**else**  
     Set  $Y = m^q + \sigma(\text{Id} - 2ee^\top)Z$ .  
**end if**  
**return**  $(X, Y, \text{bool})$  where  $Y \sim q$ .

tance ratio when using an independent draft model, in Section 4.2.

#### 4.1. Complexity analysis

We analyze here the computational benefits of using speculative sampling for DDMs under a simplified computational model. We assume an independent draft model  $p$  given by (4). The cost of evaluating  $b_t^q$  and  $b_t^p$  are  $C_q$  and  $C_p$  respectively with  $C_q > C_p$ . Using a window size  $L$ , each step of speculative sampling increases the iteration index  $n$  by a random variable  $\hat{L} \in \{1, \dots, L\}$ . The cost of running the target model for  $K$  iterations is  $C_{\text{original}} = KC_q$ , while speculative sampling approximately requires  $C_{\text{spec}} = (K/\hat{L})(LC_p + C_q)$ . This simplified computational model leads directly to the following proposition.

**Proposition 4.1 (Average cost ratio):** *We have that*

$$\mathbb{E}[C_{\text{original}}/C_{\text{spec}}] = \frac{\mathbb{E}[\hat{L}]}{1 + LC_p/C_q}. \quad (8)$$

Note that the average cost ratio (8) is independent of  $K$ . Speculative sampling is beneficial if this ratio exceeds one, which occurs if and only if

$$\mathbb{E}[\hat{L}]/L \geq C_p/C_q + 1/L. \quad (9)$$

Under the simplifying assumption that the acceptance probability of any draft state is  $\alpha$ , independent across the state sequence, one has

$$\mathbb{E}[\hat{L}] = \sum_{\ell=0}^{L-1} (\ell+1)\alpha^\ell(1-\alpha) + L\alpha^L = 1 - \alpha^L + L\alpha^{L+1}.$$

This highlights the competing factors in speculative sampling. To satisfy (9), we aim for  $\mathbb{E}[\hat{L}]/L$  to be as close to one as possible, indicating a high acceptance ratio and thus

a draft model that closely approximates the target model. This typically implies that  $C_p \approx C_q$ . Conversely, while (9) is made easier to satisfy by minimizing  $C_p/C_q$ , this will in practice cause the acceptance ratio to deteriorate, consequently decreasing  $\mathbb{E}[\hat{L}]/L$ .

#### 4.2. Lower bound on acceptance ratio

We shed light here on how the acceptance ratio depends on the problem parameters. Assume we are at step  $n$  in the speculative sampling process and let  $a_n = \mathcal{N}(Z + \Delta_n; 0, \text{Id})/\mathcal{N}(Z; 0, \text{Id})$  for  $Z \sim \mathcal{N}(0, \text{Id})$  where

$$\|\Delta_n\|^2 = \frac{1}{4}\gamma\left(\varepsilon + \frac{1}{\varepsilon}\right)^2 g_{1-t_n}^2 \|s_{1-t_n}^p(\tilde{Y}_n) - s_{1-t_n}^q(\tilde{Y}_n)\|^2,$$

for  $b_t^q(x) = -f_{1-t}x + \frac{1+\varepsilon^2}{2}g_{1-t}^2s_{1-t}^q(x)$ , i.e.  $s_t^q \approx s_t$  and similarly  $s_t^p \approx s_t$ . The draft state at time  $n+1$  is accepted if  $U \leq \min(1, a_n)$ . We have the following lower bound.

**Lemma 4.2 (Control of acceptance ratio):** *We have*

$$\mathbb{E}[a_n] \geq \exp\left[-\frac{1}{8}\gamma\left(\varepsilon + \frac{1}{\varepsilon}\right)^2 g_{1-t_n}^2\right] \times \mathbb{E}\left[\|s_{1-t_n}^p(\tilde{Y}_n) - s_{1-t_n}^q(\tilde{Y}_n)\|^2\right].$$

Next, we assume that both the draft and target models have access to exact scores, i.e., we neglect neural network approximations. However, the draft model is trained using  $p_{\text{data}}$  while the target model is trained with  $q_{\text{data}}$ . We obtain the following result.

**Theorem 4.3 (Control of acceptance ratio (II)):** *Under assumptions on  $p_{\text{data}}$  and  $q_{\text{data}}$  detailed in the supplementary material, we have*

$$\mathbb{E}[a_n] \geq \exp\left[-C\gamma g_{s_n}^2\left(\varepsilon + \frac{1}{\varepsilon}\right)^2\right] \times \min\left(\left(\frac{1}{\sigma_{s_n}} - \sigma_{s_n}\right)^2 + \alpha_{s_n}^2, \frac{1}{\alpha_{s_n}^2}D(p_{\text{data}}, q_{\text{data}})\right),$$

where  $s_n = 1 - t_n$ ,  $C$  a constant and  $D(p_{\text{data}}, q_{\text{data}})$  is some divergence between  $p_{\text{data}}$  and  $q_{\text{data}}$  explicit in the proof.

There are different factors influencing the lower bound of Theorem 4.3:

- As  $\gamma \rightarrow 0$ , we have  $\mathbb{E}[a_n] \geq 1$ , implying that a smaller discretization step size leads to higher acceptance rates of draft states. However, a smaller step size also necessitates a larger total number of steps to reach the target.
- If  $D(p_{\text{data}}, q_{\text{data}}) \rightarrow 0$  then  $\mathbb{E}[a_n] \geq 1$ . This means that if the draft and target models approximate the same data distribution then we obtain a higher acceptance rate.
- If  $g_t^2\left(\left(\frac{1}{\sigma_t} - \sigma_t\right)^2 + \alpha_t^2\right) \rightarrow 0$  as  $t \rightarrow 1$  then  $\mathbb{E}[a_n] \geq 1$  for  $n$  close to 0. This is the case for classical schedules  $(f_t, g_t)$  used in practice. Hence at the beginning of the denoising process, the acceptance rate is high.

- The dependency with respect to  $\varepsilon$  as both low and high values worsen the lower bound. There exists an optimal parameter  $\varepsilon$  ( $\varepsilon = 1.0$  in this bound). In practice, we sweep over  $\varepsilon > 0$ .

## 5. Related works

**Speculative sampling.** Introduced in the context of LLMs by Leviathan et al. (2023); Chen et al. (2023), speculative sampling relies on a draft model based on a cheap LLM. An early drafting methodology proposing multiple tokens at once was put forth by Stern et al. (2018), while drafting with independent models was explored in (Chen et al., 2023; Leviathan et al., 2023; Spector & Re, 2023; Sun et al., 2023; Christopher et al., 2024). Efficient drafting using the target model with additional feedforward neural network (FFN) heads was considered in (Stern et al., 2018; Sun et al., 2021; Xia et al., 2023; Cai et al., 2024). Finally, it has been proposed very recently by Christopher et al. (2024) to use a discrete DDM (Austin et al., 2021; Campbell et al., 2022; Lou et al., 2024) as draft model for an autoregressive target model. For a comprehensive review of speculative sampling techniques, we refer to Xia et al. (2024).

**Acceleration of diffusion models.** One line of work investigates distilling a teacher DDM into a student DDM for faster sampling; see (Luhman & Luhman, 2021; Salimans & Ho, 2022; Berthelot et al., 2023; Liu et al., 2023; Meng et al., 2023; Sauer et al., 2023; Song et al., 2023; Katzir et al., 2024; Kim et al., 2024; Xu et al., 2024; Yin et al., 2024). For a review of distillation methods, we refer to Luo (2023); Dieleman (2024). Another line of work pursues accelerating sampling through improved integrators (Dockhorn et al., 2022; Liu et al., 2022; Lu et al., 2022; Xiao et al., 2022; Zhang & Chen, 2023). Additionally, parallel sampling of DDMs has been explored in (Shih et al., 2023; Chen et al., 2024; Li et al., 2024a; Ma et al., 2024; Tang et al., 2024). Our approach complements these approaches and can be combined with parallel sampling and/or better integrators.

## 6. Experiments

In all of our experiments we track two different types of metrics. First, we assess the quality of the output distribution obtained with the speculative sampling strategy (Wasserstein-2 in the low dimensional case, FID (Heusel et al., 2017) and IS (Salimans et al., 2016) in the image experiments and reward (Chi et al., 2023) in the robotics setting). We also report the Number of Function Evaluations of the target models, i.e., the number of calls to the (expensive) target model.

**Low dimensional experiments.** We first investigate Algorithm 3 in a low dimensional setting in order to better un-

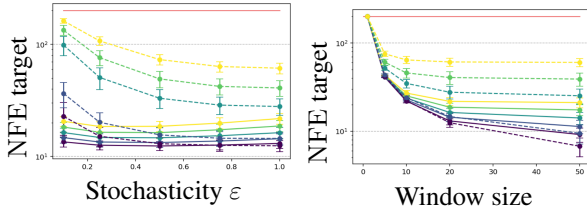


Figure 3. In each figure, the  $y$  axis corresponds to the number of evaluations of the target model. Without speculative sampling, we evaluate the target model with 200 steps and show the improvements obtained using our approach. Each dotted line corresponds to INDEPENDENT drafting, each solid line to FROZEN drafting. The color gradient purple to yellow corresponds to different dimensions of the target distribution [2, 4, 8, 16, 32].

derstand the effect of key hyperparameters of the algorithm. We consider a mixture of Gaussians target distribution with dimension varying between [2, 4, 8, 16, 32] and 16 components. All diffusion models are trained with a velocity objective, see Appendix I.1. We consider two drafting strategies: the INDEPENDENT strategy and the FROZEN strategy as described in Section 3.1. We also refer to Appendix I.1 for the architectural details. In Figure 3, we display the effects on the performance of the algorithm of the stochasticity  $\varepsilon$  in the sampler and the window size  $L$ .

Figure 3 illustrate that FROZEN drafting is more efficient than INDEPENDENT drafting as it provides a better reduction of the NFE of the target models. This is in accordance with findings in speculative decoding/sampling for LLMs, see e.g. (Cai et al., 2024). Regarding the amount of stochasticity  $\varepsilon$ , there appears to be an optimal value  $\varepsilon$  for which the speculative sampling gains are optimal in agreement with theoretical insights derived in Theorem 4.3. Finally, increasing the window size  $L$  improves the performance of speculative sampling.

**Image space experiments.** Next, we demonstrate speculative sampling in higher dimensional settings on three datasets: CIFAR10 ( $32 \times 32 \times 3$ ) and LSUN ( $64 \times 64 \times 3$ ). In all settings, the backbone architecture is a U-Net. We refer to Appendix I.1 for architectural and training details. For all experiments we report FID score computed on 50k training samples. Our results are reported in Table 1. We investigate the effect of temperature on our models. More precisely, we introduce an hyperparameter  $\tau > 0$  such that  $\mathcal{N}(Z + \Delta; 0, \text{Id})/\mathcal{N}(Z; 0, \text{Id})$  is replaced by  $\mathcal{N}(Z + \Delta; 0, \tau \text{Id})/\mathcal{N}(Z; 0, \tau \text{Id})$ , see Appendix F.1 for more details. Note that upon choosing  $\tau > 1$  we do not sample exactly from  $q$  but improve the acceptance rate. We sweep over the values of  $\varepsilon$  and  $\tau$  in Table 1 on the CIFAR10 dataset. The main conclusion is that our proposed speculative sampling algorithm provides a significant speed-up (x2 to x3) while maintaining the quality of the target model.

Configuration	Draft (100 steps)		Target (100 steps)		Target (30 steps)		Speculative		
	FID ↓	IS ↑	FID ↓	IS ↑	FID ↓	IS ↑	FID ↓	IS ↑	NFE ↓
$\varepsilon = 0.01, \tau = 0.5$	<b>17.05</b>	<b>8.67</b>	2.86	10.10	<b>4.32</b>	10.83	2.84	10.11	65.36
$\varepsilon = 0.01, \tau = 1.0$	<b>17.05</b>	<b>8.67</b>	2.86	10.10	<b>4.32</b>	10.83	2.84	10.11	61.64
$\varepsilon = 0.01, \tau = 2.0$	<b>17.05</b>	<b>8.67</b>	2.86	10.10	<b>4.32</b>	10.83	2.83	10.12	57.47
$\varepsilon = 0.25, \tau = 0.5$	81.58	7.60	<b>2.45</b>	10.31	7.68	11.32	2.42	10.24	42.44
$\varepsilon = 0.25, \tau = 1.0$	81.58	7.60	<b>2.45</b>	10.31	7.68	11.32	2.35	10.25	39.31
$\varepsilon = 0.25, \tau = 2.0$	81.58	7.60	<b>2.45</b>	10.31	7.68	11.32	<b>2.34</b>	10.32	<b>35.40</b>
$\varepsilon = 0.5, \tau = 0.5$	115.57	5.25	2.81	10.72	10.28	<b>11.55</b>	2.71	10.59	43.08
$\varepsilon = 0.5, \tau = 1.0$	115.57	5.25	2.81	10.72	10.28	<b>11.55</b>	2.71	10.57	40.37
$\varepsilon = 0.5, \tau = 2.0$	115.57	5.25	2.81	10.72	10.28	<b>11.55</b>	2.74	10.52	36.72
$\varepsilon = 1.0, \tau = 0.5$	188.29	2.64	7.09	<b>11.22</b>	28.93	11.48	7.12	11.14	46.54
$\varepsilon = 1.0, \tau = 1.0$	188.29	2.64	7.09	<b>11.22</b>	28.93	11.48	7.10	<b>11.18</b>	44.81
$\varepsilon = 1.0, \tau = 2.0$	188.29	2.64	7.09	<b>11.22</b>	28.93	11.48	7.11	11.14	42.11

Table 1. CIFAR-10 evaluation. For each column, we report the best result in **bold**.

Configuration	Target		Speculative	
	Reward ↑	NFE ↓	Reward ↑	NFE ↓
$L = 20, K = 100$	$0.889 \pm 0.008$	100	$0.898 \pm 0.008$	$27.245 \pm 0.002$
$L = 20, K = 80$	$0.882 \pm 0.008$	80	$0.899 \pm 0.008$	$23.890 \pm 0.003$
$L = 20, K = 40$	$0.898 \pm 0.008$	40	$0.875 \pm 0.008$	$15.544 \pm 0.005$
$L = 20, K = 20$	$0.887 \pm 0.008$	20	$0.901 \pm 0.008$	$9.430 \pm 0.004$
$L = 10, K = 10$	$0.901 \pm 0.008$	10	$0.903 \pm 0.007$	$5.053 \pm 0.001$
$L = 5, K = 5$	$0.876 \pm 0.008$	5	$0.870 \pm 0.009$	$3.000 \pm 0.000$

Table 2. PushT evaluation.

For example, on CIFAR10, we reach a FID score of 2.34 with only 35 calls to the target model, while the classical sampling procedure requires 100 calls to the target model to reach a FID score of 2.45, which represents a reduction of 65% of the number of calls to the target model. Running the target model for only 30 steps on the other hand reduces the image quality, as the FID score worsens to 4.32. It is worth noting that increasing the temperature marginally improve FID and IS score for some values of  $\varepsilon$ . We observe similar improvements (around halving the NFE) in the case of LSUN, see Appendix J.

**PushT dataset.** Finally, we conclude our experimental study by showing that speculative sampling also yields improvements for a robotics task, where the policy is generated using a diffusion model following (Chi et al., 2023). In our setting, we focus on the PushT dataset, where the goal for the robot is to push a T shape object on a corresponding area. The state space is of dimension  $(16, 2)$ , where 16 corresponds to the prediction horizon and 2 is the dimension of the action. We refer to Appendix I.1 for more details. The metric we report is the reward  $r \in [0, 1]$  where  $r = 1.0$  means that the policy achieves perfect coverage over an episode. For robustness we run 1000 episodes to compute the mean of the maximum rewards. For each episode we run the policy for 300 steps or stop if we reach the maximum reward. We follow the setting of (Chi et al., 2023), see also Appendix I.1. For our speculative sampler we fix  $\tau = 1$  and do not perform any parallel call. We only consider the FROZEN drafting strategy. We report our results in Table 2.

We consistently observe that the speculative sampling strategy reduces the number of call to the target models while preserving the quality of the model. For instance, with only 5 calls to the target model, our speculative sampler achieves a reward of  $0.903 \pm 0.007$  while running the target model with only 5 steps yield a reward of  $0.876 \pm 0.008$ .

## 7. Discussion

We have developed here a novel speculative sampling procedure to accelerate diffusion models. This was achieved by exploiting the connections between speculative sampling and maximal coupling, specifically through the use of reflection maximal coupling. Note that this procedure is not restricted to DDMs and can be applied to accelerate the simulation of any time-discretized diffusion process with a computationally expensive drift term. We have demonstrated that significant speed-up can be achieved while sampling exactly from the target distribution.

This approach has some limitations. Speculative sampling is not applicable to deterministic samplers, although noise can be added in a principled way to such samplers to obtain a valid stochastic sampler, to which speculative sampling can then be applied (see e.g. Section 3.1). Another limitation, shared with Picard iteration techniques (Shih et al., 2023; Chen et al., 2024), is the increased memory overhead due to the parallel calls to the sampler during the verification procedure.



## References

- Albergo, M. S., Boffi, N. M., and Vanden-Eijnden, E. Stochastic interpolants: A unifying framework for flows and diffusions. *arXiv preprint arXiv:2303.08797*, 2023.
- Austin, J., Johnson, D. D., Ho, J., Tarlow, D., and Van Den Berg, R. Structured denoising diffusion models in discrete state-spaces. In *Advances in Neural Information Processing Systems*, 2021.
- Berthelot, D., Autef, A., Lin, J., Yap, D. A., Zhai, S., Hu, S., Zheng, D., Talbott, W., and Gu, E. Tract: Denoising diffusion models with transitive closure time-distillation. *arXiv preprint arXiv:2303.04248*, 2023.
- Bou-Rabee, N., Eberle, A., and Zimmer, R. Coupling and convergence for Hamiltonian Monte Carlo. *The Annals of Applied Probability*, 30(3):1209–1250, 2020.
- Cai, T., Li, Y., Geng, Z., Peng, H., Lee, J. D., Chen, D., and Dao, T. Medusa: Simple LLM inference acceleration framework with multiple decoding heads. In *International Conference on Machine Learning*, 2024.
- Campbell, A., Benton, J., De Bortoli, V., Rainforth, T., Deligiannidis, G., and Doucet, A. A continuous time framework for discrete denoising models. In *Advances in Neural Information Processing Systems*, 2022.
- Chen, C., Borgeaud, S., Irving, G., Lespiau, J.-B., Sifre, L., and Jumper, J. Accelerating large language model decoding with speculative sampling. *arXiv preprint arXiv:2302.01318*, 2023.
- Chen, H., Ren, Y., Ying, L., and Rotskoff, G. M. Accelerating diffusion models with parallel sampling: Inference at sub-linear time complexity. In *Advances in Neural Information Processing Systems*, 2024.
- Chi, C., Feng, S., Du, Y., Xu, Z., Cousineau, E., Burchfiel, B., and Song, S. Diffusion policy: Visuomotor policy learning via action diffusion. *arXiv preprint arXiv:2303.04137*, 2023.
- Christopher, J. K., Bartoldson, B. R., Kailkhura, B., and Fioretto, F. Speculative diffusion decoding: Accelerating language generation through diffusion. *arXiv preprint arXiv:2408.05636*, 2024.
- De Bortoli, V., Hutchinson, M., Wirnsberger, P., and Doucet, A. Target score matching. *arXiv preprint arXiv:2402.08667*, 2024.
- Del Moral, P. *Feynman-Kac Formulae: Genealogical and Interacting Particle Approximations*. Springer, 2004.
- Dieleman, S. The paradox of diffusion distillation, 2024. URL <https://sander.ai/2024/02/28/paradox.html>.
- Dockhorn, T., Vahdat, A., and Kreis, K. Genie: Higher-order denoising diffusion solvers. *Advances in Neural Information Processing Systems*, 2022.
- Doucet, A., De Freitas, N., and Gordon, N. J. *Sequential Monte Carlo Methods in Practice*. Information Science and Statistics. New York, NY: Springer, New York, 2001.
- Esser, P., Rombach, R., and Ommer, B. Taming transformers for high-resolution image synthesis. In *Proceedings of the IEEE/CVF conference on Computer Vision and Pattern Recognition*, 2021.
- Esser, P., Kulal, S., Blattmann, A., Entezari, R., Müller, J., Saini, H., Levi, Y., Lorenz, D., Sauer, A., Boesel, F., Podell, D., Dockhorn, T., English, Z., Lacey, K., Goodwin, A., Marek, Y., and Rombach, R. Scaling rectified flow transformers for high-resolution image synthesis. In *International Conference on Machine Learning*, 2024.
- Heusel, M., Ramsauer, H., Unterthiner, T., Nessler, B., and Hochreiter, S. Gans trained by a two time-scale update rule converge to a local Nash equilibrium. In *Advances in Neural Information Processing Systems*, 2017.
- Higgins, I., Matthey, L., Pal, A., Burgess, C. P., Glorot, X., Botvinick, M. M., Mohamed, S., and Lerchner, A. beta-vae: Learning basic visual concepts with a constrained variational framework. In *International Conference on Learning Representations*, 2016.
- Ho, J., Jain, A., and Abbeel, P. Denoising diffusion probabilistic models. In *Advances in Neural Information Processing Systems*, 2020.
- Hsu, E. P. and Sturm, K.-T. Maximal coupling of Euclidean Brownian motions. *Communications in Mathematics and Statistics*, 1:93–104, 2013.
- Jacob, P. Lectures on Couplings and Monte Carlo. <https://sites.google.com/site/pierrejacob/cmclecures>, 2021.
- Karras, T., Aittala, M., Aila, T., and Laine, S. Elucidating the design space of diffusion-based generative models. In *Advances in Neural Information Processing Systems*, 2022.
- Karras, T., Aittala, M., Kynkäänniemi, T., Lehtinen, J., Aila, T., and Laine, S. Guiding a diffusion model with a bad version of itself. In *Advances in Neural Information Processing Systems*, 2024.
- Katzir, O., Patashnik, O., Cohen-Or, D., and Lischinski, D. Noise-free score distillation. In *International Conference on Learning Representations*, 2024.

- Kim, D., Lai, C.-H., Liao, W.-H., Murata, N., Takida, Y., Uesaka, T., He, Y., Mitsufuji, Y., and Ermon, S. Consistency trajectory models: Learning probability flow ODE trajectory of diffusion. In *International Conference on Learning Representations*, 2024.
- Kingma, D. P. and Welling, M. Auto-encoding variational Bayes. *International Conference on Learning Representations*, 2014.
- Leviathan, Y., Kalman, M., and Matias, Y. Fast inference from transformers via speculative decoding. In *International Conference on Machine Learning*, 2023.
- Li, M., Cai, T., Cao, J., Zhang, Q., Cai, H., Bai, J., Jia, Y., Li, K., and Han, S. Distrifusion: Distributed parallel inference for high-resolution diffusion models. In *Proceedings of the IEEE/CVF Conference on Computer Vision and Pattern Recognition*, 2024a.
- Li, T., Tian, Y., Li, H., Deng, M., and He, K. Autoregressive image generation without vector quantization. In *Advances in Neural Information Processing Systems*, 2024b.
- Lindvall, T. *Lectures on the Coupling Method*. John Wiley & Sons, New York, 1992.
- Liu, L., Ren, Y., Lin, Z., and Zhao, Z. Pseudo numerical methods for diffusion models on manifolds. In *International Conference on Learning Representations*, 2022.
- Liu, X., Zhang, X., Ma, J., Peng, J., and Liu, Q. InstafLOW: One step is enough for high-quality diffusion-based text-to-image generation. In *International Conference on Learning Representations*, 2023.
- Lou, A., Meng, C., and Ermon, S. Discrete diffusion language modeling by estimating the ratios of the data distribution. In *International Conference on Machine Learning*, 2024.
- Lu, C., Zhou, Y., Bao, F., Chen, J., Li, C., and Zhu, J. Dpm-solver: A fast ODE solver for diffusion probabilistic model sampling in around 10 steps. In *Advances in Neural Information Processing Systems*, 2022.
- Luhman, E. and Luhman, T. Knowledge distillation in iterative generative models for improved sampling speed. *arXiv preprint arXiv:2101.02388*, 2021.
- Luo, W. A comprehensive survey on knowledge distillation of diffusion models. *arXiv preprint arXiv:2304.04262*, 2023.
- Ma, X., Fang, G., and Wang, X. Deepcache: Accelerating diffusion models for free. In *Proceedings of the IEEE/CVF Conference on Computer Vision and Pattern Recognition*, 2024.
- Meng, C., Rombach, R., Gao, R., Kingma, D., Ermon, S., Ho, J., and Salimans, T. On distillation of guided diffusion models. In *Proceedings of the IEEE/CVF Conference on Computer Vision and Pattern Recognition*, 2023.
- Rombach, R., Blattmann, A., Lorenz, D., Esser, P., and Ommer, B. High-resolution image synthesis with latent diffusion models. In *Proceedings of the IEEE/CVF Conference on Computer Vision and Pattern Recognition*, 2022.
- Salimans, T. and Ho, J. Progressive distillation for fast sampling of diffusion models. In *International Conference on Learning Representations*, 2022.
- Salimans, T., Goodfellow, I., Zaremba, W., Cheung, V., Radford, A., and Chen, X. Improved techniques for training GANs. *Advances in Neural Information Processing Systems*, 2016.
- Sauer, A., Lorenz, D., Blattmann, A., and Rombach, R. Adversarial diffusion distillation. *arXiv preprint arXiv:2311.17042*, 2023.
- Shih, A., Belkale, S., Ermon, S., Sadigh, D., and Anari, N. Parallel sampling of diffusion models. In *Advances in Neural Information Processing Systems*, 2023.
- Shoji, I. and Ozaki, T. Estimation for nonlinear stochastic differential equations by a local linearization method. *Stochastic Analysis and Applications*, 16(4):733–752, 1998.
- Sohl-Dickstein, J., Weiss, E., Maheswaranathan, N., and Ganguli, S. Deep unsupervised learning using nonequilibrium thermodynamics. In *International Conference on Machine Learning*, 2015.
- Song, J., Meng, C., and Ermon, S. Denoising diffusion implicit models. In *International Conference on Learning Representations*, 2021.
- Song, Y., Dhariwal, P., Chen, M., and Sutskever, I. Consistency models. In *International Conference on Machine Learning*, 2023.
- Spector, B. F. and Re, C. Accelerating LLM inference with staged speculative decoding. In *Workshop on Efficient Systems for Foundation Models@ ICML2023*, 2023.
- Stern, M., Shazeer, N., and Uszkoreit, J. Blockwise parallel decoding for deep autoregressive models. In *Advances in Neural Information Processing Systems*, 2018.
- Sun, X., Ge, T., Wei, F., and Wang, H. Instantaneous grammatical error correction with shallow aggressive decoding. In *Proceedings of the 59th Annual Meeting of the Association for Computational Linguistics and the 11th International Joint Conference on Natural Language Processing*

- (Volume 1: Long Papers). Association for Computational Linguistics, 2021.
- Sun, Z., Suresh, A. T., Ro, J. H., Beirami, A., Jain, H., and Yu, F. Spectr: Fast speculative decoding via optimal transport. In *Advances in Neural Information Processing Systems*, 2023.
- Tang, Z., Tang, J., Luo, H., Wang, F., and Chang, T.-H. Accelerating parallel sampling of diffusion models. In *International Conference on Machine Learning*, 2024.
- Thorisson, H. *Coupling, Stationarity, and Regeneration*. Springer, New York, 2000.
- Vincent, P. A connection between score matching and denoising autoencoders. *Neural Computation*, 23(7):1661–1674, 2011.
- Wang, Z., Zhang, R., Ding, K., Yang, Q., Li, F., and Xiang, S. Continuous speculative decoding for autoregressive image generation. In *Advances in Neural Information Processing Systems*, 2024.
- Xia, H., Ge, T., Wang, P., Chen, S.-Q., Wei, F., and Sui, Z. Speculative decoding: Exploiting speculative execution for accelerating seq2seq generation. In *Findings of the Association for Computational Linguistics: EMNLP 2023*, pp. 3909–3925, 2023.
- Xia, H., Yang, Z., Dong, Q., Wang, P., Li, Y., Ge, T., Liu, T., Li, W., and Sui, Z. Unlocking efficiency in large language model inference: A comprehensive survey of speculative decoding. *arXiv preprint arXiv:2401.07851*, 2024.
- Xiao, Z., Kreis, K., and Vahdat, A. Tackling the generative learning trilemma with denoising diffusion gans. In *International Conference on Learning Representations*, 2022.
- Xu, Y., Zhao, Y., Xiao, Z., and Hou, T. Ufogen: You forward once large scale text-to-image generation via diffusion GANs. In *Proceedings of the IEEE/CVF Conference on Computer Vision and Pattern Recognition*, 2024.
- Yin, T., Gharbi, M., Zhang, R., Shechtman, E., Durand, F., Freeman, W. T., and Park, T. One-step diffusion with distribution matching distillation. In *Proceedings of the IEEE/CVF Conference on Computer Vision and Pattern Recognition*, 2024.
- Zhang, Q. and Chen, Y. Fast sampling of diffusion models with exponential integrator. In *International Conference on Learning Representations*, 2023.
- Zhang, R., Isola, P., Efros, A. A., Shechtman, E., and Wang, O. The unreasonable effectiveness of deep features as a perceptual metric. In *Proceedings of the IEEE/CVF Conference on Computer Vision and Pattern Recognition*, 2018.

## Organization of the Supplementary Material

This supplementary material is organized as follows. Proofs of the main results are gathered in Appendix A. Potential alternative drafting strategies are discussed in Appendix B. A detailed implementation of speculative sampling for diffusion models is presented in Appendix C. An extension of the maximal coupling strategy for Gaussian with different variances is proposed in Appendix E. In Appendix F, we investigate different acceptance strategies in the case of Gaussian speculative sampling. Appendix G presents an extension of speculative sampling to incorporate some spatial transform. In Appendix H, we establish a lower bound on the expectation of the log-acceptance ratio. Experimental details are gathered in Appendix I.

### A. Proofs of the Main Results

#### A.1. Proof of Proposition 2.1

The joint distribution of  $(X, Y)$  generated by Algorithm 2 is

$$f(x, y) = p(x)(\alpha(x)\delta_x(y) + (1 - \alpha(x))r(y)),$$

with  $\delta_x(y)$  the Kronecker-delta symbol and  $\alpha(x) = \min(1, q(x)/p(x))$ . That is we first sample  $X \sim p$  then set  $Y = X$  with probability  $\alpha(X)$  and sample  $Y \sim r$  otherwise. It follows that the marginal distribution of  $Y$  is given by

$$f(y) = \sum_{x \in \mathcal{X}} f(x, y) = \alpha(y)p(y) + \left(1 - \sum_{x \in \mathcal{X}} \alpha(x)p(x)\right)r(y). \quad (10)$$

We have

$$\begin{aligned} r(y) &\propto \max(0, q(y) - p(y)) \\ &= q(y) - \min(p(y), q(y)) \\ &= q(y) - \alpha(y)p(y). \end{aligned}$$

Therefore, we have that

$$r(y) = \frac{q(y) - \alpha(y)p(y)}{1 - \sum_{x \in \mathcal{X}} \alpha(x)p(x)}.$$

Hence, by substituting the expression of  $r(y)$  in (10), we obtain  $f(y) = q(y)$ , that is  $Y \sim q$ . Now by construction, we have that

$$\begin{aligned} \mathbb{P}(X \neq Y) &= 1 - \sum_{x \in \mathcal{X}} p(x)\alpha(x) \\ &= 1 - \sum_{x \in \mathcal{X}} \min(p(x), q(x)) \\ &= \|p - q\|_{\text{TV}}, \end{aligned}$$

as  $\min(a, b) = \frac{1}{2}(a + b - |a - b|)$  for any  $a, b$ . However, Lindvall's inequality (Lindvall, 1992) (also known as the coupling inequality) shows that any pair of random variables  $X, Y$  satisfying marginally  $X \sim p$  and  $Y \sim q$  verify

$$\|p - q\|_{\text{TV}} \leq \mathbb{P}(X \neq Y). \quad (11)$$

Algorithm 2 generates a joint distribution for which the inequality (11) becomes an equality; hence it is optimal.

#### A.2. Proof of Proposition 3.1

It is clear that Algorithm 4 outputs  $X \sim \mathcal{N}(m^p; \sigma^2 \text{Id})$ . We check here that the algorithm also returns  $Y \sim \mathcal{N}(m^q; \sigma^2 \text{Id})$ . To show this, we leverage the fact that we can rewrite  $Y = m^q + \sigma \tilde{Z}$  for some random variable  $\tilde{Z}$  whose distribution follows

$$\begin{aligned} f(\tilde{z}) &= \int \delta_{z+\Delta}(\tilde{z}) \min\left(1, \frac{\mathcal{N}(z+\Delta; 0, \text{Id})}{\mathcal{N}(z; 0, \text{Id})}\right) \mathcal{N}(z; 0, \text{Id}) dz \\ &\quad + \int \delta_{(\text{Id}-2ee^\top)_z}(\tilde{z}) \max\left(0, 1 - \frac{\mathcal{N}(z+\Delta; 0, \text{Id})}{\mathcal{N}(z; 0, \text{Id})}\right) \mathcal{N}(z; 0, \text{Id}) dz, \end{aligned}$$



where we have used  $1 - \min(1, a) = \max(0, 1 - a)$  for  $a \geq 0$ . Hence to show the validity of the procedure, we need now to show that  $\tilde{Z} \sim \mathcal{N}(0, \text{Id})$ , i.e.,  $f(\tilde{z}) = \mathcal{N}(\tilde{z}; 0, \text{Id})$ . We have

$$\begin{aligned} & \int \delta_{z+\Delta}(\tilde{z}) \min\left(1, \frac{\mathcal{N}(z+\Delta; 0, \text{Id})}{\mathcal{N}(z; 0, \text{Id})}\right) \mathcal{N}(z; 0, \text{Id}) dz \\ &= \int \delta_{z+\Delta}(\tilde{z}) \min\left(\mathcal{N}(z; 0, \text{Id}), \mathcal{N}(z+\Delta; 0, \text{Id})\right) dz \\ &= \min\left(\mathcal{N}(\tilde{z}-\Delta; 0, \text{Id}), \mathcal{N}(\tilde{z}; 0, \text{Id})\right). \end{aligned}$$

In addition, we have that

$$\begin{aligned} & \int \delta_{(\text{Id}-2ee^\top)z}(\tilde{z}) \max\left(0, 1 - \frac{\mathcal{N}(z+\Delta; 0, \text{Id})}{\mathcal{N}(z; 0, \text{Id})}\right) \mathcal{N}(z; 0, \text{Id}) dz \\ &= \int \delta_{(\text{Id}-2ee^\top)z}(\tilde{z}) \max\left(0, \mathcal{N}(z; 0, \text{Id}) - \mathcal{N}(z+\Delta; 0, \text{Id})\right) dz \\ &= \max\left(0, \mathcal{N}((\text{Id}-2ee^\top)\tilde{z}; 0, \text{Id}) - \mathcal{N}((\text{Id}-2ee^\top)\tilde{z}+\Delta; 0, \text{Id})\right) \\ &= \max\left(0, \mathcal{N}(\tilde{z}; 0, \text{Id}) - \mathcal{N}(\tilde{z}-\Delta; 0, \text{Id})\right) \end{aligned}$$

as  $\tilde{z} = (\text{Id} - 2ee^\top)z$  implies that  $z = (\text{Id} - 2ee^\top)\tilde{z}$  and  $\mathcal{N}((\text{Id} - 2ee^\top)\tilde{z}; 0, \text{Id}) = \mathcal{N}(\tilde{z}; 0, \text{Id})$  because  $\|(\text{Id} - 2ee^\top)\tilde{z}\| = \|\tilde{z}\|$ . Finally we used the fact that  $\mathcal{N}((\text{Id} - 2ee^\top)\tilde{z} + \Delta; 0, \text{Id}) = \mathcal{N}(\tilde{z} - \Delta; 0, \text{Id})$  as

$$\begin{aligned} \|(\text{Id} - 2ee^\top)\tilde{z} + \Delta\|^2 &= \|\Delta\|^2 + \|(\text{Id} - 2ee^\top)\tilde{z}\|^2 + 2\Delta^\top \tilde{z} - 4\Delta^\top ee^\top \tilde{z} \\ &= \|\Delta\|^2 + \|\tilde{z}\|^2 - 2\Delta^\top \tilde{z} \\ &= \|\tilde{z} - \Delta\|^2, \end{aligned}$$

as  $ee^\top = \Delta\Delta^\top / \|\Delta\|^2$ . Combining these results, we obtain that

$$\begin{aligned} f(\tilde{z}) &= \min(\mathcal{N}(\tilde{z}-\Delta; 0, \text{Id}), \mathcal{N}(\tilde{z}; 0, \text{Id})) + \max(0, \mathcal{N}(\tilde{z}; 0, \text{Id}) - \mathcal{N}(\tilde{z}-\Delta; 0, \text{Id})) \\ &= \mathcal{N}(\tilde{z}; 0, \text{Id}). \end{aligned}$$

We thus have proved that  $\tilde{Z} \sim \mathcal{N}(0, \text{Id})$ , so  $Y \sim \mathcal{N}(m^q, \sigma^2 \text{Id})$ . To prove now this coupling is a maximal coupling, we compute  $\mathbb{P}(X \neq Y)$ . Recall that  $X = Y$  if  $U \leq \min(1, \mathcal{N}(z+\Delta; 0, \text{Id})/\mathcal{N}(z; 0, \text{Id}))$  so

$$\mathbb{P}(X \neq Y) = 1 - \int \min\left(\mathcal{N}(z; 0, \text{Id}), \mathcal{N}(z+\Delta; 0, \text{Id})\right) dz.$$

It is straightforward to check that this is indeed equal to

$$\|p - q\|_{\text{TV}} = \|\mathcal{N}(\mu_1, \sigma^2 \text{Id}) - \mathcal{N}(\mu_2, \sigma^2 \text{Id})\|_{\text{TV}} = 2\Phi(\|\Delta\|/2) - 1,$$

where  $\Phi$  is the cumulative distribution function of the standard normal random variable. Hence, it follows from Lindvall's inequality (Lindvall, 1992) that Algorithm 4 outputs a maximal coupling.

### A.3. Optimality of reflection maximal coupling

In Appendix A.2 we have shown that the reflection coupling is a maximal coupling. In what follows, we denote  $\mathcal{C}(m^p, m^q)$  the set of coupling, i.e., distributions on  $\mathbb{R}^d \times \mathbb{R}^d$  with marginals  $\mathcal{N}(m^p, \sigma^2 \text{Id})$  and  $\mathcal{N}(m^q, \sigma^2 \text{Id})$ . We also denote  $\Pi_{\text{reflection}} \in \mathcal{C}(m^p, m^q)$  the reflection coupling. Proposition 3.1 shows that

$$\Pi_{\text{reflection}} \in \operatorname{argmin}_{\Pi \in \mathcal{C}(m^p, m^q)} \mathbb{E}_{(X, Y) \sim \Pi} [\mathbf{1}_{X \neq Y}].$$

In fact, Hsu & Sturm (2013, Theorem 4.2) show that

$$\Pi_{\text{reflection}} \in \operatorname{argmin}_{\Pi \in \mathcal{C}(m^p, m^q)} \mathbb{E}_{(X, Y) \sim \Pi} [\phi(\|X - Y\|)],$$

for every non-negative, strictly increasing and strictly concave function  $\phi$  with  $\phi(0) = 0$ . Hence, the reflection coupling also naturally appears if one considers other cost functions than  $(x, y) \mapsto \mathbf{1}_{x \neq y}$ .

## B. Alternative drafting strategies for diffusion models

**Medusa-like correction.** To improve the frozen target as draft model (see (5)), we can introduce a correction term to the frozen model. Our correction is inspired by the Medusa architecture (Cai et al., 2024). More precisely, we consider a smaller *correction model*  $c_{s,t}^\theta$  trained with the following loss

$$\mathcal{L}(\theta) = \int_0^1 \int_0^1 \|b_t^q(x_t) - b_s^q(x_s) - c_{s,t}^\theta(x_s, x_t)\|^2 p_{s,t}(x_s, x_t) dx_s dx_t. \quad (12)$$

Here  $p_{s,t}$  can be any distribution on  $\mathbb{R}^d$  as the minimizer for  $c_{s,t}(x_s, x_t)$  is always  $b_t^q(x_t) - b_s^q(x_s)$ . However, in practice, one may choose  $p_{s,t}(x_s, x_t)$  such that for  $s > t$ ,  $(\mathbf{X}_t, \mathbf{X}_s) \sim p$  with

$$\mathbf{X}_t = \alpha_t \mathbf{X}_0 + \sigma_t \mathbf{Z}_t, \quad \mathbf{X}_s = \frac{\alpha_t}{\alpha_s} \mathbf{X}_s + (\sigma_t^2 - (\frac{\sigma_s \alpha_t}{\alpha_s})^2)^{1/2} \mathbf{Z}_s,$$

where  $\mathbf{Z}_t$  and  $\mathbf{Z}_s$  are independent Gaussian random variables with zero mean and identity covariance matrix. It can be shown that in that case  $\mathbf{X}_s$  and  $\mathbf{X}_t$  are on trajectory of

$$d\mathbf{X}_u = f_u \mathbf{X}_u + g_u d\mathbf{B}_u.$$

If the correction model is expressive enough then the minimizer of (12) is given by  $c_{s,t}^\theta(x_s, x_t) = b_t^q(x_t) - b_s^q(x_s)$  and in that case the draft model is equal to the target model.

We then have a model  $p(y_k | y_{n:k-1}) = \mathcal{N}(y_k; m_{k-1}^p(y_{n:k-1}), \sigma_{k-1}^2 \text{Id})$  with

$$m_k^p(y_{n:k}) = y_k + \gamma \{b_{t_n}^q(y_n) + c_{t_n, t_k}^\theta(y_n, y_k)\}, \quad \sigma_k = \varepsilon \sqrt{\gamma} g_{1-t_k}.$$

Hence, on a window of size  $L$ , we only need to evaluate the target model once while the (cheap) correction model is evaluated  $L$  times. If  $c_{s,t}^\theta = 0$  then we recover the draft model proposed in (5). Note that similarly to the frozen model, we can sample the draft states in parallel.

**Combining draft models.** Assume we have  $N_p$  draft models such that  $p_\ell(y_k | y_{k-1}) = \mathcal{N}(y_k; m_{k-1}^{p,\ell}(y_{n:k-1}), \sigma_{k-1}^2 \text{Id})$  and let  $\alpha_{k-1}^\ell(y_{k-1}) \geq 0$  such that  $\sum_{\ell=1}^{N_p} \alpha_{k-1}^\ell(y_{k-1}) = 1$ . We can define a new draft distribution

$$p_{\text{mix}}^\alpha(y_k | y_{k-1}) = \mathcal{N}(y_k; m_{k-1}^{\text{mix}}(y_{k-1}), \sigma_{k-1}^2 \text{Id}), \quad m_{k-1}^{\text{mix}}(y_{k-1}) = \sum_{\ell=1}^{N_p} \alpha_{k-1}^\ell(y_{k-1}) m_{k-1}^{p,\ell}(y_{k-1}). \quad (13)$$

The distribution in (13) mixes together  $N_p$  draft models by considering a convex combination of their means. Since it is a Gaussian, Section 3.3 applies and we get that

$$\mathbb{P}(Y_k \neq \tilde{Y}_k | Y_{k-1}) = 2\Phi(\sigma^{-1} \|m^p(\cdot | Y_{k-1}) - m_{k-1}^{\text{mix}}(Y_{k-1})\|/2) - 1,$$

The parameters,  $\alpha_k(y_{n-1})$  can either be hyperparameters (constants) specified by the practitioner, or can be represented by a mapping  $\alpha_k^\ell(y_k; \theta)$  with parameters  $\theta$ . These parameters  $\theta$  can be learned by minimizing the sum of average rejection probabilities  $\mathbb{E}_{Y_{0:K} \sim q} \left[ \sum_{k=1}^K \mathbb{P}(Y_k \neq \tilde{Y}_k | Y_{k-1}) \right]$ .

**Parallel sampling and speculative correction.** We know show how one can combine Picard iterations from ParaDiGMS (Shih et al., 2023) and speculative sampling. We start by recalling the Picard iterations from Shih et al. (2023). Consider a draft sequence initialized with  $\tilde{Y}_{n+1:n_L}^0$  where  $n_L = \max(K, n + L)$  such that  $\tilde{Y}_{n+1:n_L}^0 = F(\tilde{Y}_n)$ . Then, we define the Picard iterations as

$$\tilde{Y}_k^m = \tilde{Y}_{k-1}^{m-1} + \gamma \bar{b}_{t_{k-1}}^q(\tilde{Y}_{k-1}^{m-1}), \quad \tilde{Y}_n^m = \tilde{Y}_n.$$

where  $k \in \{n+1, \dots, n_L\}$  and  $m \in \{1, \dots, M-1\}$ , we consider a *deterministic* sampler, here we set  $\varepsilon = 0$  in  $\bar{b}_{t_k}$ , see (1). Hence, for any  $k \in \{n+1, \dots, n_L\}$  there exists a function  $F_k^m$  such that

$$\tilde{Y}_k^m = F_k^m(\tilde{Y}_n).$$

Lastly, we consider a last Picard iteration

$$\tilde{Y}_k^M = \tilde{Y}_{k-1}^{M-1} + \gamma b_{t_{k-1}}^q(\tilde{Y}_{k-1}^{M-1}) + \varepsilon \sqrt{\gamma} g_{t_{k-1}} Z_k,$$

where  $Z_{k-1} \sim \mathcal{N}(0, \text{Id})$ . Hence, we have

$$\tilde{Y}_k^M = F_{k-1}^{M-1}(\tilde{Y}_n) + \gamma b_{t_{k-1}}^q(F_{k-1}^{M-1}(\tilde{Y}_n)) + \varepsilon \sqrt{\gamma} \sigma_{t_{k-1}} Z_k.$$

We consider the sequence  $\tilde{Y}_{n+1:n_L}^M$  as a draft sequence. In that case we still have that  $\tilde{Y}_{n+1:n_L}^M \sim p(y_{n+1:n_L} | y_n)$  with

$$p(y_{n+1:n_L} | y_n) = \prod_{k=n+1}^{n_L} p(y_k | y_{n:k-1}) = \prod_{k=n+1}^{n_L} \mathcal{N}(y_k; m_{k-1}^p(y_{n:k-1}), \sigma_{k-1}^2 \text{Id}),$$

and

$$m_k^p(y_{n:k-1}) = F_k^{M-1}(y_n) + \gamma b_{t_k}(F_k^{M-1}(y_n)), \quad \sigma_k = \varepsilon \sqrt{\gamma} g_{t_k}.$$

### C. Detailed implementation of speculative sampling for diffusion models

We present in Algorithm 5 a detailed implementation of speculative sampling for diffusion models, an algorithm combining Algorithm 3 and Algorithm 4.

---

#### Algorithm 5 Speculative Sampling for DDM

---

**Require:** Lookahead integer  $L$ , sequence length  $K$ , target model  $q$  (see eq. (2)) and draft model  $p$  (see eq. (3)).

Sample  $Y_0 \sim \mathcal{N}(0, \text{Id})$  and set  $n = 0$ .

**while**  $n < K$  **do**

    Set  $\tilde{Y}_n \leftarrow Y_n$  and  $n_L = \min(n + L, K)$ .

**for**  $k = n + 1 : n_L$  **do**

        Sample  $\tilde{Y}_k \sim \mathcal{N}(m_{k-1}^p(\tilde{Y}_{n:k-1}), \sigma_{k-1}^2 \text{Id})$ .

**end for**

    In parallel, compute  $m_n^q(\tilde{Y}_n), m_{n+1}^q(\tilde{Y}_{n+1}), \dots, m_{n_L-1}^q(\tilde{Y}_{n_L-1})$ .

**for**  $k = n + 1 : n_L$  **do**

        Set  $\Delta_{k-1} = (m_{k-1}^p(\tilde{Y}_{n:k-1}) - m_{k-1}^q(\tilde{Y}_{k-1})) / \sigma_{k-1}$  and  $e = \Delta_{k-1} / \|\Delta_{k-1}\|$ .

        Let  $Z_{k-1} = (\tilde{Y}_k - m_{k-1}^p(\tilde{Y}_{n:k-1})) / \sigma_{k-1}$ .

        Sample  $U \sim \text{Unif}[0, 1]$ .

**bool** =  $\mathbb{I}[U \leq \min(1, \mathcal{N}(Z_{k-1} + \Delta_{k-1}; 0, \text{Id}) / \mathcal{N}(Z_{k-1}; 0, \text{Id}))]$ .

**if** **bool** **then**

            Set  $Y_k = \tilde{Y}_k$ .

**else**

            Set  $Y_k = m_{k-1}^q(\tilde{Y}_{k-1}) + \sigma_{k-1}(\text{Id} - 2ee^\top)Z_{k-1}$ .

**end if**

**return**  $(Y_k, \text{bool})$ .

**if** **not**(**bool**) **then**

            Exit For Loop

**end if**

**end for**

    Set  $n \leftarrow t$ .

**end while**

**return**  $Y_K$

---

### D. Distribution of time to rejection

Consider the following process  $(\tilde{Y}_k, Y_k)_{k \geq 0}$  following the following distribution

$$\Gamma(\tilde{y}_{0:n}, y_{0:n}) = p(\tilde{y}_0) \delta_{\tilde{y}_0}(y_0) \prod_{k=1}^n p(\tilde{y}_k | y_{k-1}) \left( \alpha_k(y_{k-1}, \tilde{y}_k) \delta_{\tilde{y}_k}(y_k) + (1 - \alpha_k(y_{k-1}, \tilde{y}_k)) r(y_k | y_{k-1}, \tilde{y}_k) \right).$$

where

$$\alpha_k(y_{k-1}, \tilde{y}_k) = \min\left(1, \frac{q(\tilde{y}_k|y_{k-1})}{p(\tilde{y}_k|y_{k-1})}\right)$$

and

$$r(y_k|y_{k-1}, \tilde{y}_k) = \delta_{f(y_{k-1}, \tilde{y}_k)}(y_k)$$

corresponds to reflection maximal coupling. This distribution describes the speculative sampling algorithm for diffusions (not describing the drafting process over an horizon of  $L$  but this is irrelevant). By construction, we have  $\int \Gamma(\tilde{y}_{0:n}, y_{0:n}) d\tilde{y}_{0:n} = q(y_{0:n})$ . Starting from  $\tilde{Y}_0 = Y_0$ , we can look at the first time  $\tau$ ,  $\tau \geq 1$ , the draft state is rejected. This is equivalent to look at the first time that  $\tilde{Y}_k \neq Y_k$ . We have from direct calculations that

$$\mathbb{P}(\tau > k) = \int \cdots \int p(\tilde{y}_{0:k}) \prod_{i=1}^k \alpha_i(\tilde{y}_{i-1}, \tilde{y}_i) d\tilde{y}_{0:k}.$$

Hence  $\mathbb{P}(\tau > k)$  is given by a Feynman-Kac formula (Del Moral, 2004). This shows in particular that we could simply estimate this quantity by running a particle filter (Del Moral, 2004; Doucet et al., 2001). A similar expression can be obtained for the distribution of  $\tau_n$  the  $n^{\text{th}}$  time the draft state is rejected starting from the last time one rejected a draft,  $p(\tilde{y}_0)$  being replaced by  $p(\tilde{y}_{\tau_{n-1}+1}|y_{\tau_n})$ .

In the simplifying case where we have

$$p(y_k|y_{k-1}) = \mathcal{N}(y_k; y_{k-1} + \gamma b^p(y_{k-1}), \gamma \text{Id}), \quad q(y_k|y_{k-1}) = \mathcal{N}(y_k; y_{k-1} + \gamma b^q(y_{k-1}), \gamma \text{Id}).$$

Under the assumption that  $\|b^p(x) - b^q(x)\| \geq M$ , we have

$$\begin{aligned} \alpha_{\gamma,k} &= \mathbb{P}(\tilde{Y}_0 = Y_0) \prod_{i=1}^k \mathbb{P}(\tilde{Y}_i = Y_i | \tilde{Y}_{i-1} = Y_{i-1}) \\ &= \prod_{i=1}^k 2\Phi\left(-\sqrt{\gamma} \|b^p(Y_{i-1}) - b^q(Y_{i-1})\|/2\right) \\ &\leq (2\Phi(-\sqrt{\gamma}M/2))^k. \end{aligned}$$

We have  $2\Phi(-x) = 1 - \sqrt{\frac{2}{\pi}}x + o(x^3)$  so

$$\lim_{\gamma \rightarrow 0} \alpha_{\gamma,1/\gamma} = 0.$$

## E. Maximal coupling between Gaussian distributions with different covariance

Algorithm 4 is restricted to Gaussian random variables with same covariance matrix. This implies that the draft and the target samplers introduce the same amount of noise at each step. One can wonder if the two samplers can have different noise levels. In the following examples, we show that even in a simple Gaussian setting the probability of rejection in that case is extremely high as the dimension increases.

Indeed, consider two centered  $d$ -dimensional normals  $p(x) = \mathcal{N}(x; 0, \sigma_1^2 \text{Id})$  and  $q(x) = \mathcal{N}(x; 0, \sigma_2^2 \text{Id})$ . We assume that  $\sigma_2 < \sigma_1$ . In that case, we have that  $p(x) \leq q(x)$  if and only if  $\|x\|^2 \leq R^2$  with

$$R^2 = d \log(\sigma_1^2/\sigma_2^2) (1/\sigma_2^2 - 1/\sigma_1^2)^{-1}.$$

Hence, in the ideal case where the acceptance probability  $r$  is given by  $\|p - q\|_{\text{TV}}$ , we get that

$$r = 1 - \mathbb{E}[\mathbf{1}_{\sigma_1^2 Q \leq R^2}] - \mathbb{E}[\mathbf{1}_{\sigma_2^2 Q \geq R^2}] = \mathbb{E}[\mathbf{1}_{Q \leq R^2/\sigma_2^2}] - \mathbb{E}[\mathbf{1}_{Q \leq R^2/\sigma_1^2}].$$

where  $Q$  is a  $\chi^2$  random variable with  $d$  degrees of freedom. Unfortunately this probability is extremely close to 0 as  $d$  increases, see Figure 4. Therefore, there is no hope to maximally couple two samplers with different noise levels at scale.



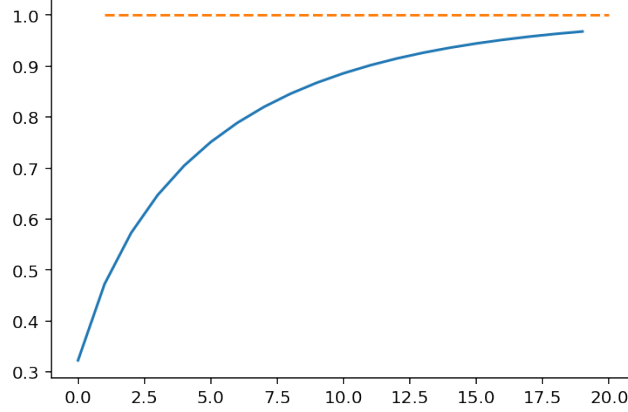


Figure 4. Evolution of the rejection probability ( $y$ -axis) with the dimension ( $x$ -axis) for  $\sigma_1 = 0.2$  and  $\sigma_2 = 0.1$

## F. Alternative verification strategies

In this section, we investigate different verification strategies for Algorithm 4. First, we introduce a temperature parameter in Appendix F.1. Then, in Appendix F.2, we adapt the *typical acceptance* criterion of Stern et al. (2018); Cai et al. (2024) to our setting.

### F.1. Influence of the temperature

Consider Algorithm 6, which is a version of Algorithm 4 including an additional temperature parameter.

---

**Algorithm 6** (Temperature) REJECTION ( $p, q, X$ ) for two Gaussians with same covariance

---

**Require:** Probability densities  $p(x) = \mathcal{N}(x; m^p, \sigma^2 \text{Id})$ ,  $q(x) = \mathcal{N}(x; m^q, \sigma^2 \text{Id})$ ,  $X \sim p$ ,  $\tau > 0$ .

Set  $\Delta = (m^p - m^q)/\sigma$  and  $e = \Delta/||\Delta||$ .

Let  $Z = (X - m^p)/\sigma$ .

Sample  $U \sim \text{Unif}[0, 1]$ .

$\text{bool} = \mathbb{I}[U \leq \min(1, \mathcal{N}(Z + \Delta; 0, \tau \text{Id})/\mathcal{N}(Z; 0, \tau \text{Id}))]$ .

**if**  $\text{bool}$  **then**

    Set  $Y = X$ .

**else**

    Set  $Y = m^q + \sigma(\text{Id} - 2ee^\top)Z$ .

**end if**

**return**  $(X, Y, \text{bool})$ .

---

Setting  $\tau = 1$ , we recover Algorithm 4 but for  $\tau > 1$  we have a larger probability of accepting the current proposal  $X$ . This higher acceptance rate, of course, is not without its drawbacks since we are no longer sampling from the correct distribution. In what follows, we analyze how the distribution is shifted when tuning the temperature parameter  $\tau > 0$ . To shorten notation, we use in the following proof the notation  $\varphi_\tau(z) = \mathcal{N}(z; 0, \tau \text{Id})$  and  $\varphi = \varphi_1$  for  $\tau = 1$ . We recall that  $C_c(\mathbb{R}^d)$  is the set of continuous functions with compact support. For any  $f \in C_c(\mathbb{R}^d)$ , using that for any  $x \in \mathbb{R}^d$ ,  $\|x\| = \|\hat{x}\|$  for

$\hat{x} = (\text{Id} - 2ee^\top)x$ , and  $x \mapsto (\text{Id} - 2ee^\top)x$  is an involution, we have

$$\begin{aligned}
 \mathbb{E}[f(Y)] &= \int_{\mathbb{R}^d} f(m^p + \sigma z) \min(1, \varphi_\tau(z + \Delta)/\varphi_\tau(z)) \varphi(z) dz \\
 &\quad + \int_{\mathbb{R}^d} f(m^q + \sigma \hat{z}) (1 - \min(1, \varphi_\tau(z + \Delta)/\varphi_\tau(z))) \varphi(z) dz, \\
 &= \int_{\mathbb{R}^d} f(m^p + \sigma z) \min(1, \varphi_\tau(z + \Delta)/\varphi_\tau(z)) \varphi(z) dz \\
 &\quad + \int_{\mathbb{R}^d} f(m^q + \sigma z) (1 - \min(1, \varphi_\tau(\hat{z} + \Delta)/\varphi_\tau(z))) \varphi(z) dz, \\
 &= \int_{\mathbb{R}^d} f(m^p + \sigma z) \min(1, \varphi_\tau(z + \Delta)/\varphi_\tau(z)) \varphi(z) dz \\
 &\quad - \int_{\mathbb{R}^d} f(m^q + \sigma z) \min(1, \varphi_\tau(\hat{z} + \Delta)/\varphi_\tau(z)) \varphi(z) dz, \\
 &\quad + \int_{\mathbb{R}^d} f(m^q + \sigma z) \varphi(z) dz \\
 &= \int_{\mathbb{R}^d} f(m^q + \sigma z) \min(1, \varphi_\tau(z)/\varphi_\tau(z - \Delta)) \varphi(z - \Delta) dz \\
 &\quad - \int_{\mathbb{R}^d} f(m^q + \sigma z) \min(1, \varphi_\tau(\hat{z} + \Delta)/\varphi_\tau(z)) \varphi(z) dz, \\
 &\quad + \int_{\mathbb{R}^d} f(m^q + \sigma z) \varphi(z) dz.
 \end{aligned}$$

We have that  $\widehat{\hat{z} + \Delta} = z - \Delta$ . Hence, we get that

$$\begin{aligned}
 \mathbb{E}[f(Y)] &= \int_{\mathbb{R}^d} f(m^q + \sigma z) \min(1, \varphi_\tau(z)/\varphi_\tau(z - \Delta)) \varphi(z - \Delta) dz \\
 &\quad - \int_{\mathbb{R}^d} f(m^q + \sigma z) \min(1, \varphi_\tau(\hat{z} + \Delta)/\varphi_\tau(z)) \varphi(z) dz, \\
 &\quad + \int_{\mathbb{R}^d} f(m^q + \sigma z) \varphi(z) dz \\
 &= \int_{\mathbb{R}^d} f(m^q + \sigma z) \min(\varphi(z - \Delta)/\varphi(z), (\varphi_\tau(z)\varphi(z - \Delta))/(\varphi_\tau(z - \Delta)\varphi(z))) \varphi(z) dz \\
 &\quad - \int_{\mathbb{R}^d} f(m^q + \sigma z) \min(1, \varphi_\tau(\hat{z} + \Delta)/\varphi_\tau(z)) \varphi(z) dz, \\
 &\quad + \int_{\mathbb{R}^d} f(m^q + \sigma z) \varphi(z) dz \\
 &= \int_{\mathbb{R}^d} f(m^q + \sigma z) \min(\varphi(z - \Delta)/\varphi(z), (\varphi_\tau(z)\varphi(z - \Delta))/(\varphi_\tau(z - \Delta)\varphi(z))) \varphi(z) dz \\
 &\quad - \int_{\mathbb{R}^d} f(m^q + \sigma z) \min(1, \varphi_\tau(z - \Delta)/\varphi_\tau(z)) \varphi(z) dz, \\
 &\quad + \int_{\mathbb{R}^d} f(m^q + \sigma z) \varphi(z) dz.
 \end{aligned}$$

Hence, we get that

$$\mathbb{E}[f(Y)] = \int_{\mathbb{R}^d} f(m^q + \sigma z) (1 + a_\tau(z)) \varphi(z) dz, \tag{14}$$

where

$$a_\tau(z) = -\min(1, \varphi_\tau(z - \Delta)/\varphi_\tau(z)) + \min((\varphi_\tau(z)\varphi(z - \Delta))/(\varphi_\tau(z - \Delta)\varphi(z)), \varphi(z - \Delta)/\varphi(z)).$$

Note that for  $\tau = 1$  we have that  $a_\tau(z) = 0$ . If we let  $\tau \rightarrow +\infty$  then we get that  $a_\tau(z) = -1 + \varphi(z - \Delta)/\varphi(z)$  so  $Y \sim \mathcal{N}(m^p, \sigma^2 \text{Id})$  from (14), i.e., we always accept the draft model. In Figure 5, we show the effect of the temperature on the output distribution. The influence of the temperature in more realistic settings is studied in Appendix I.

**Link with guidance.** We first the following result and subsequently explain its connections with (Karras et al., 2024).

**Proposition F.1 (Link with guidance):** *Let  $(X, Y)$  be the output of Algorithm 6. We have that*

$$\mathbb{E}[Y] = m^q + (1/\sigma)C_\tau(\|\Delta\|)(m^p - m^q),$$

*with  $\Delta = (m^p - m^q)/\sigma$  and  $C_\tau(\|\Delta\|) \leq 0$  if  $\tau \leq 1$  and  $C_\tau(\|\Delta\|) \geq 0$  otherwise. In particular, we have that  $C_\tau(\|\Delta\|) = 0$  if  $\tau = 1$ . In addition,  $C_\tau(\|\Delta\|)$  is explicit in the proof.*

Before giving the proof of this result let us give some interpretation. For  $\tau = 1$ , we recover that the proposed mechanism is a coupling and that  $Y$  has the correct target distribution and in particular the mean is the mean of the target distribution. For  $\tau > 1$ , we raise the acceptance ratio: this has the effect of moving the distribution of  $Y$  towards the distribution of  $X$ . Looking at the mean, we can interpret this effect has a guidance effect, where we push towards  $m^p$  and away for  $m^q$ . For  $\tau < 1$ , we are pushing towards the target distribution even more than with  $\tau = 1$ . Looking at the mean of  $Y$  we can interpret this effect as a guidance term, i.e., pushing away from the draft model and towards the target model. This last setting is similar to (Karras et al., 2024), which consider an explicit guidance of a "good" model with a "bad" model.

*Proof.* Using (14), we have that

$$\begin{aligned} \mathbb{E}[Y] &= \int_{\mathbb{R}^d} (m^q + \sigma z)(1 + a_\tau(z))\varphi(z)dz \\ &= m^q + m^q \int_{\mathbb{R}^d} a_\tau(z)\varphi(z)dz + \sigma \int_{\mathbb{R}^d} z a_\tau(z)\varphi(z)dz. \end{aligned}$$

First, we show that  $\int_{\mathbb{R}^d} a_\tau(z)dz = 0$ . Indeed, using the change of variable  $z \mapsto -z$  and  $z \mapsto z - \Delta$  we get

$$\begin{aligned} \int_{\mathbb{R}^d} a_\tau(z)\varphi(z)dz &= \int_{\mathbb{R}^d} \min((\varphi_\tau(z)\varphi(z - \Delta))/(\varphi_\tau(z - \Delta)\varphi(z)), \varphi(z - \Delta)/\varphi(z))\varphi(z)dz \\ &\quad - \int_{\mathbb{R}^d} \min(1, \varphi_\tau(z - \Delta)/\varphi_\tau(z))\varphi(z)dz \\ &= \int_{\mathbb{R}^d} \min((\varphi_\tau(z)\varphi(z + \Delta))/(\varphi_\tau(z + \Delta)\varphi(z)), \varphi(z + \Delta)/\varphi(z))\varphi(z)dz \\ &\quad - \int_{\mathbb{R}^d} \min(1, \varphi_\tau(z - \Delta)/\varphi_\tau(z))\varphi(z)dz \\ &= \int_{\mathbb{R}^d} \min((\varphi_\tau(z - \Delta)\varphi(z))/(\varphi_\tau(z)\varphi(z - \Delta)), \varphi(z)/\varphi(z - \Delta))\varphi(z - \Delta)dz \\ &\quad - \int_{\mathbb{R}^d} \min(1, \varphi_\tau(z - \Delta)/\varphi_\tau(z))\varphi(z)dz \\ &= \int_{\mathbb{R}^d} \min((\varphi_\tau(z - \Delta)\varphi(z))/\varphi_\tau(z), \varphi(z))dz \\ &\quad - \int_{\mathbb{R}^d} \min(\varphi(z), \varphi(z)\varphi_\tau(z - \Delta)/\varphi_\tau(z))dz = 0. \end{aligned}$$

Hence, we have that

$$\mathbb{E}[Y] = \int_{\mathbb{R}^d} (m^q + \sigma z)(1 + a_\tau(z))\varphi(z)dz = m^q + \sigma \int_{\mathbb{R}^d} z a_\tau(z)\varphi(z)dz.$$

We are going to show that

$$\int_{\mathbb{R}^d} \langle z, e \rangle a_\tau(z)\varphi(z)dz = 0,$$

where we recall that  $e = \Delta / \|\Delta\|$ . For any  $z \in \mathbb{R}^d$ , we have that  $z = z_e e + \sum_{i=1}^{d-1} z_{e_i} e_i$ , where  $z_e = \langle z, e \rangle$  and  $z_{e_i} = \langle z, e_i \rangle$  with  $\{e, e_i\}_{i=1}^{d-1}$  an orthonormal basis. Note in particular that for any  $i \in \{1, \dots, d-1\}$ ,  $\langle e_i, \Delta \rangle = 0$ . We have that

$$\begin{aligned}
 \int_{\mathbb{R}^d} z a_\tau(z) \varphi(z) dz &= \int_{\mathbb{R}^d} z \min((\varphi_\tau(z) \varphi(z - \Delta)) / (\varphi_\tau(z - \Delta) \varphi(z)), \varphi(z - \Delta) / \varphi(z)) \varphi(z) dz \\
 &\quad - \int_{\mathbb{R}^d} z \min(1, \varphi_\tau(z - \Delta) / \varphi_\tau(z)) \varphi(z) dz \\
 &= \int_{\mathbb{R}^d} z \min(\varphi_\tau(z) \varphi(z - \Delta) / \varphi_\tau(z - \Delta), \varphi(z - \Delta)) dz \\
 &\quad - \int_{\mathbb{R}^d} z \min(\varphi(z), \varphi_\tau(z - \Delta) \varphi(z) / \varphi_\tau(z)) dz \\
 &= - \int_{\mathbb{R}^d} (z - \Delta) \min(\varphi_\tau(z - \Delta) \varphi(z) / \varphi_\tau(z), \varphi(z)) dz \\
 &\quad - \int_{\mathbb{R}^d} z \min(\varphi(z), \varphi_\tau(z - \Delta) \varphi(z) / \varphi_\tau(z)) dz \\
 &= -2 \int_{\mathbb{R}^d} z \min(\varphi_\tau(z - \Delta) \varphi(z) / \varphi_\tau(z), \varphi(z)) dz \\
 &\quad + \Delta \int_{\mathbb{R}^d} \min(\varphi_\tau(z - \Delta) \varphi(z) / \varphi_\tau(z), \varphi(z)) dz. \tag{15}
 \end{aligned}$$

Next, we look at  $z \mapsto \min(\varphi_\tau(z - \Delta) \varphi(z) / \varphi_\tau(z), \varphi(z))$ . For any  $z$ , let  $z_{e^\perp} = z - z_e e$ . Note that  $\langle z_{e^\perp}, \Delta \rangle = 0$ . We have that

$$\begin{aligned}
 &\min(\varphi_\tau(z - \Delta) \varphi(z) / \varphi_\tau(z), \varphi(z)) \\
 &= \min(\varphi_\tau(z_e - \|\Delta\|) \varphi_\tau(z_{e^\perp}) \varphi(z_e) \varphi(z_{e^\perp}) / (\varphi_\tau(z_e) \varphi_\tau(z_{e^\perp})), \varphi(z_e) \varphi(z_{e^\perp})) \\
 &= \min(\varphi_\tau(z_e - \|\Delta\|) \varphi(z_e) \varphi(z_{e^\perp}) / \varphi_\tau(z_e), \varphi(z_e) \varphi(z_{e^\perp})) \\
 &= \varphi(z_{e^\perp}) \min(\varphi_\tau(z_e - \|\Delta\|) \varphi(z_e) / \varphi_\tau(z_e), \varphi(z_e)).
 \end{aligned}$$

Using this result, (15) and the fact that for any  $i \in \{1, \dots, d-1\}$ ,  $\langle e_i, \Delta \rangle = 0$ , we get

$$\left\langle \int_{\mathbb{R}^d} z a_\tau(z) \varphi(z) dz, e_i \right\rangle = 0.$$

Therefore, we get that

$$\mathbb{E}[Y] = m^q + (1/\sigma) C_\tau(\|\Delta\|) (m^p - m^q).$$

In the rest of the proof, we give an explicit expression for the parameter  $C_\tau(\Delta)$ . We first find  $z$  such that  $\varphi_\tau(z_e - \|\Delta\|) \varphi(z_e) / \varphi_\tau(z_e) \leq \varphi(z_e)$ , i.e., we find  $z$  such that  $\log(\varphi_\tau(z_e - \|\Delta\|)) \leq \log(\varphi_\tau(z_e))$ , i.e.,  $z_e \leq \|\Delta\|/2$ . In particular, we have that

$$\begin{aligned}
 &\int_{\mathbb{R}} \min(\varphi_\tau(z_e - \|\Delta\|) \varphi(z_e) / \varphi_\tau(z_e), \varphi(z_e)) dz_e \\
 &= \int_{-\infty}^{\|\Delta\|/2} \varphi(z_e) dz_e + \int_{\|\Delta\|/2}^{+\infty} \varphi_\tau(z_e - \|\Delta\|) \varphi(z_e) / \varphi_\tau(z_e) dz_e \\
 &= \Phi(\|\Delta\|/2) + \int_{\|\Delta\|/2}^{+\infty} \varphi_\tau(z_e - \|\Delta\|) \varphi(z_e) / \varphi_\tau(z_e) dz_e.
 \end{aligned}$$

In addition, we have that

$$\varphi_\tau(z_e - \|\Delta\|) \varphi(z_e) / \varphi_\tau(z_e) = \varphi(z_e - \|\Delta\|/\tau) \exp[\|\Delta\|^2/\tau^2(1-\tau)].$$

Therefore, we get that

$$\begin{aligned}
 &\int_{\mathbb{R}} \min(\varphi_\tau(z_e - \|\Delta\|) \varphi(z_e) / \varphi_\tau(z_e), \varphi(z_e)) dz_e \\
 &= \Phi(\|\Delta\|/2) + \exp[\|\Delta\|^2/\tau^2(1-\tau)] (1 - \Phi(\|\Delta\|(\frac{1}{2} - \frac{1}{\tau}))) \\
 &= \Phi(\|\Delta\|/2) + \exp[\|\Delta\|^2/\tau^2(1-\tau)] \Phi(\|\Delta\|(\frac{1}{\tau} - \frac{1}{2})). \tag{16}
 \end{aligned}$$



Similarly, we have that

$$\begin{aligned}
 & \int_{\mathbb{R}} z_e \min(\varphi_{\tau}(z_e - \|\Delta\|)\varphi(z_e)/\varphi_{\tau}(z_e), \varphi(z_e)) dz_e \\
 &= \int_{-\infty}^{\|\Delta\|/2} z_e \varphi(z_e) dz_e + \int_{\|\Delta\|/2}^{+\infty} z_e \varphi_{\tau}(z_e - \|\Delta\|)\varphi(z_e)/\varphi_{\tau}(z_e) dz_e \\
 &= \int_{-\infty}^{\|\Delta\|/2} z_e \varphi(z_e) dz_e + \exp[\|\Delta\|^2/\tau^2(1-\tau)] \int_{\|\Delta\|/2}^{+\infty} z_e \varphi(z_e - \|\Delta\|/\tau) dz_e \\
 &= \int_{-\infty}^{\|\Delta\|/2} z_e \varphi(z_e) dz_e + \exp[\|\Delta\|^2/\tau^2(1-\tau)] \int_{\|\Delta\|/2}^{+\infty} (z_e - \Delta)\varphi(z_e - \|\Delta\|/\tau) dz_e \\
 &\quad + \|\Delta\| \int_{\|\Delta\|/2}^{+\infty} \exp[\|\Delta\|^2/\tau^2(1-\tau)] \varphi(z_e - \|\Delta\|/\tau) dz_e \\
 &= \varphi(\|\Delta\|(\frac{1}{2} - \frac{1}{\tau})) - \varphi(\|\Delta\|/2) + \|\Delta\| \int_{\|\Delta\|/2}^{+\infty} \exp[\|\Delta\|^2/\tau^2(1-\tau)] \varphi(z_e - \|\Delta\|/\tau) dz_e \\
 &= \varphi(\|\Delta\|(\frac{1}{\tau} - \frac{1}{2})) - \varphi(\|\Delta\|/2) + \|\Delta\| \exp[\|\Delta\|^2/\tau^2(1-\tau)] \Phi(\|\Delta\|(\frac{1}{\tau} - \frac{1}{2})). \tag{17}
 \end{aligned}$$

Combining (16), (17) and (15), we get that

$$\begin{aligned}
 \left\langle e, \int_{\mathbb{R}^d} z a_{\tau}(z) dz \right\rangle &= -2\varphi(\|\Delta\|(\frac{1}{\tau} - \frac{1}{2})) + 2\varphi(\|\Delta\|/2) \\
 &\quad - 2 \exp[\|\Delta\|^2/\tau^2(1-\tau)] \|\Delta\| \Phi(\|\Delta\|(\frac{1}{\tau} - \frac{1}{2})) + \|\Delta\| \Phi(\|\Delta\|/2) \\
 &\quad + \|\Delta\| \exp[\|\Delta\|^2/\tau^2(1-\tau)] \Phi(\|\Delta\|(\frac{1}{\tau} - \frac{1}{2})) \\
 &= -2\varphi(\|\Delta\|(\frac{1}{\tau} - \frac{1}{2})) + 2\varphi(\|\Delta\|/2) \\
 &\quad + \|\Delta\| \Phi(\|\Delta\|/2) - \|\Delta\| \exp[\|\Delta\|^2/\tau^2(1-\tau)] \Phi(\|\Delta\|(\frac{1}{\tau} - \frac{1}{2})).
 \end{aligned}$$

Therefore, we have

$$\begin{aligned}
 C_{\tau}(\|\Delta\|) &= -\frac{2}{\|\Delta\|} \varphi(\|\Delta\|(\frac{1}{\tau} - \frac{1}{2})) + \frac{2}{\|\Delta\|} \varphi(\|\Delta\|/2) \\
 &\quad + \Phi(\|\Delta\|/2) - \exp[\|\Delta\|^2/\tau^2(1-\tau)] \Phi(\|\Delta\|(\frac{1}{\tau} - \frac{1}{2})).
 \end{aligned}$$

It can be checked that  $C_{\tau}(\|\Delta\|) \leq 0$  if  $\tau \leq 1$  and  $C_{\tau}(\|\Delta\|) \geq 0$  otherwise. In particular, we have that  $C_{\tau}(\|\Delta\|) = 0$  if  $\tau = 1$ .  $\square$

## F.2. Typical acceptance in the Gaussian case

In this section, we derive the *typical acceptance* criterion introduced in (Stern et al., 2018; Cai et al., 2024). More precisely, we consider the following acceptance ration

$$a(x) = \min(1, \max(q(x)/\kappa, q(x) \exp[H(q)]/\delta)). \tag{18}$$

where  $H(q)$  is the entropy of  $q$ , i.e.,  $H(q) = -\int_{\mathbb{R}^d} q(x) \log q(x) dx$ . The hyperparameters  $\kappa, \delta > 0$  are assumed to be fixed. We recall that  $q(x) = \mathcal{N}(x; m^q, \sigma^2 \text{Id})$ . In that case we have that

$$H(q) = (d/2)(1 + \log(2\pi) + \sigma^2).$$

Hence, if we replace the acceptance criterion in Algorithm 4 with (18) and, if the sample is rejected, apply a deterministic orthogonal transformation  $z \mapsto \hat{z}$  to the Gaussian noise, we get that for any  $f \in C_c(\mathbb{R}^d)$

$$\mathbb{E}[f(Y)] = \int_{\mathbb{R}^d} [a(m^p + \sigma z) f(m^p + \sigma z) + (1 - a(m^p + \sigma z)) f(m^q + \sigma \hat{z})] \mathcal{N}(z; 0, \text{Id}) dz$$

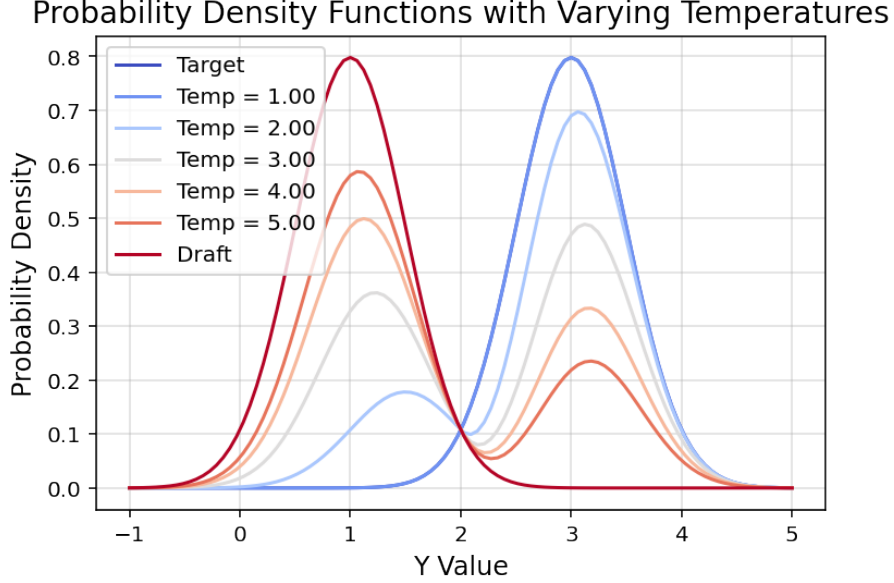


Figure 5. Effect of the temperature on the distribution of  $Y$ . Draft model has mean 1.0 and standard deviation 0.5. Target model has mean 3.0 and standard deviation 0.5.

Hence, we get

$$\begin{aligned}
 \mathbb{E}[f(Y)] &= \int_{\mathbb{R}^d} [a(m^p + \sigma z)f(m^p + \sigma z) + (1 - a(m^p + \sigma z))f(m^q + \sigma \hat{z})] \mathcal{N}(z; 0, \text{Id}) dz \\
 &= \int_{\mathbb{R}^d} [a(m^p + \sigma z)f(m^p + \sigma z) + (1 - a(m^p + \sigma \hat{z}))f(m^q + \sigma z)] \mathcal{N}(z; 0, \text{Id}) dz \\
 &= \int_{\mathbb{R}^d} \left[ \frac{\mathcal{N}(z - \Delta; 0, \text{Id})}{\mathcal{N}(z; 0, \text{Id})} a(m^q + \sigma z)f(m^q + \sigma z) + (1 - a(m^p + \sigma \hat{z}))f(m^q + \sigma z) \right] \mathcal{N}(z; 0, \text{Id}) dz \\
 &= \int_{\mathbb{R}^d} \left[ \frac{\mathcal{N}(z - \Delta; 0, \text{Id})}{\mathcal{N}(z; 0, \text{Id})} a(m^q + \sigma z) + (1 - a(m^p + \sigma \hat{z})) \right] f(m^q + \sigma z) \mathcal{N}(z; 0, \text{Id}) dz
 \end{aligned}$$

Therefore, we have

$$\mathbb{E}[f(Y)] = \int_{\mathbb{R}^d} f(m^q + \sigma z) \left( 1 + \frac{\mathcal{N}(z - \Delta; 0, \text{Id})}{\mathcal{N}(z; 0, \text{Id})} a(m^q + \sigma z) - a(m^p + \sigma \hat{z}) \right) \mathcal{N}(z; 0, \text{Id}) dz.$$

## G. Projection and extension to operators

In this section, we show that we can introduce an acceptance criterion so that two random variables are maximally coupled in a latent space. This relaxes the criterion introduced in Algorithm 4. In particular, it is possible to reach higher acceptance rate than with Algorithm 4. Of course, there is a price to pay for this increased flexibility as the variable  $Y$  does not follow the target distribution  $q$  anymore.

To start with, consider a linear operator  $A \in \mathbb{R}^{d \times d}$  such that  $AA^\top$  is invertible, i.e.,  $A$  is surjective. In Algorithm 7, we show how to maximally couple two  $d$ -dimensional densities of the form  $\mathcal{N}(x; Am^p, \sigma^2 AA^\top)$  and  $\mathcal{N}(x; Am^q, \sigma^2 AA^\top)$ .

Algorithm 7 operates directly in the “latent” space, i.e., it provides a maximal coupling  $(X_A, Y_A)$  where  $X_A \sim \mathcal{N}(Am^p, \sigma^2 AA^\top \text{Id})$  and  $Y_A \sim \mathcal{N}(Am^q, \sigma^2 AA^\top \text{Id})$ .

We now present Algorithm 8, which is a non-trivial rewriting of Algorithm 7 operating on the original  $(X, Y)$  and thus induces maximally coupled  $(X_A, Y_A)$ . In what follows, we denote  $A^\dagger$  the Moore-Penrose inverse of  $A$  defined by

$$A^\dagger = A^\top (AA^\top)^{-1}.$$

---

**Algorithm 7** REJECTION ( $p, q, X$ ) for two Gaussians with same (full) covariance
 

---

**Require:** matrix  $A$ ,  $p_A(x) = \mathcal{N}(x; Am^p, \sigma^2 AA^\top \text{Id})$ ,  $q_A(x) = \mathcal{N}(x; Am^q, \sigma^2 AA^\top \text{Id})$ ,  $X_A \sim p_A$ .  
 Set  $\Delta_A = (AA^\top)^{-1/2}A(m^p - m^q)/\sigma$  and  $e_A = \Delta_A/\|\Delta_A\|$ .  
 Let  $Z_A = (AA^\top)^{-1/2}(X_A - Am^p)/\sigma$ .  
 Sample  $U \sim \text{Unif}[0, 1]$ .  
 $\text{bool} = \mathbb{I}[U \leq \min(1, \mathcal{N}(Z_A + \Delta_A; 0, \text{Id})/\mathcal{N}(Z_A; 0, \text{Id}))]$   
**if**  $\text{bool}$  **then**  
     Set  $Y_A = X_A$ .  
**else**  
     Set  $Y_A = Am^q + \sigma(AA^\top)^{1/2}(\text{Id} - 2e_A e_A^\top)Z_A$ .  
**end if**  
**return**  $(X_A, Y_A, \text{bool})$ .

---

The validity of Algorithm 8 is based on the following lemma.

**Lemma G.1 (Latent reflection):** Let  $AA^\top$  be invertible. Let  $X = m^p + \sigma Z$  with  $Z \sim \mathcal{N}(x; 0, \text{Id})$ . Let  $Z_A = (AA^\top)^{-1/2}AZ$ . Let  $e_A = \Delta_A/\|\Delta_A\|$  where  $\Delta_A = (AA^\top)^{-1/2}A\Delta$  and  $\Delta = (m^p - m^q)/\sigma$ . We have that

$$Am^q + \sigma(AA^\top)^{1/2}(\text{Id} - 2e_A e_A^\top)Z_A = A \left[ m^q + \sigma \left( Z - 2 \frac{Z^\top A^\dagger A \Delta}{\Delta^\top A^\dagger A \Delta} \Delta \right) \right]. \quad (19)$$

In addition, we have that

$$\exp[-\frac{1}{2}(\Delta + 2Z)^\top A^\dagger A \Delta] = \mathcal{N}(Z_A + \Delta_A; 0, \text{Id})/\mathcal{N}(Z_A; 0, \text{Id}). \quad (20)$$

*Proof.* First, we have the following

$$\begin{aligned} A(m^p - m^q)(m^p - m^q)A^\dagger AZ &= (AA^\top)^{1/2}(AA^\top)^{-1/2}A(m^p - m^q)(m^p - m^q)A^\top(AA^\top)^{-1}AZ \\ &= (AA^\top)^{1/2}(AA^\top)^{-1/2}A(m^p - m^q)(m^p - m^q)A^\top(AA^\top)^{-1/2}Z_A \\ &= \sigma^2(AA^\top)^{1/2}\Delta_A\Delta_A^\top Z_A. \end{aligned}$$

Hence, we have that

$$A\Delta\Delta^\top A^\dagger AZ = (AA^\top)^{1/2}\Delta_A\Delta_A^\top Z_A. \quad (21)$$

Next, we have that for any  $u \in \mathbb{R}^d$

$$u^\top A^\dagger A u = u^\top A^\top (AA^\top)^{-1} A u = \|(AA^\top)^{-1/2} A u\|^2. \quad (22)$$

Hence, we have that

$$\Delta^\top A^\dagger A \Delta = \|(AA^\top)^{-1/2} \Delta\|^2 = \|\Delta_A\|^2.$$

Combining this result and (21), we have

$$\begin{aligned} A \left[ m^q + \sigma \left( Z - 2 \frac{Z^\top A^\dagger A \Delta}{\Delta^\top A^\dagger A \Delta} \Delta \right) \right] &= A \left[ m^q + \sigma \left( Z - 2 \frac{\Delta^\top A^\dagger A Z}{\Delta^\top A^\dagger A \Delta} \Delta \right) \right] \\ &= A \left[ m^q + \sigma \left( Z - 2 \frac{\Delta \Delta^\top}{\Delta^\top A^\dagger A \Delta} A^\dagger A Z \right) \right] \\ &= Am^q + \sigma(AA^\top)^{1/2}(\text{Id} - 2e_A e_A^\top)Z_A, \end{aligned}$$

which concludes the proof of (19). Second, we have that

$$\begin{aligned} (\Delta + 2Z)^\top A^\dagger A \Delta &= \Delta^\top A^\dagger A \Delta + Z^\top A^\dagger A \Delta + \Delta^\top A^\dagger A Z \\ &= (Z + \Delta)^\top A^\dagger A (Z + \Delta) - Z^\top A^\dagger A Z \\ &= \|(AA^\top)^{-1/2} A (Z + \Delta)\|^2 - \|(AA^\top)^{-1/2} A Z\|^2 \\ &= \|Z_A + \Delta_A\|^2 - \|Z_A\|^2, \end{aligned}$$

where we have used (22). This concludes the proof of (20).  $\square$

**Algorithm 8** REJECTION ( $p, q, X$ ) for two Gaussians with same (full) covariance

**Require:** Matrix  $A$ ,  $p(x) = \mathcal{N}(x; m^p, \sigma^2 \text{Id})$ ,  $q(x) = \mathcal{N}(x; m^q, \sigma^2 \text{Id})$ ,  $X \sim p$ .  
 $\Delta = (m^p - m^q)/\sigma$   
 Sample  $U \sim \text{Unif}[0, 1]$ .  
 $\text{bool} = \mathbb{I}[U \leq \min(1, \exp[-\frac{1}{2}(\Delta + 2Z)^\top A^\dagger A \Delta])]$   
**if**  $\text{bool}$  **then**  
     Set  $Y = X$ .  
**else**  
     Set  $Y = m^q + \sigma \left( Z - 2 \frac{Z^\top A^\dagger A \Delta}{\Delta^\top A^\dagger A \Delta} \Delta \right)$ .  
**end if**  
**return**  $(X, Y, \text{bool})$ .

The main advantage of Algorithm 8 compared to Algorithm 7 is that it only requires the knowledge of  $A$  and  $A^\dagger$  and implicitly provide a maximal coupling between  $X_A$  and  $Y_A$ . Note that if  $A$  is invertible, then we have that  $A^\dagger = A^{-1}$  and Algorithm 8 becomes identical to Algorithm 4 and thus returns a maximal coupling between  $X$  and  $Y$ . However, Algorithm 8 is also applicable when only  $AA^\top$  is invertible. In that case, we do *not* recover that  $Y \sim \mathcal{N}(x; m^q, \sigma^2 \text{Id})$  but the algorithm can still be applied and does induce maximally coupled  $(X_A, Y_A)$ .

In particular, given a mapping  $f$  and a mapping  $g$  such that  $g(f(x)) \approx x$  for  $x \in \mathbb{R}^d$ , we can define Algorithm 9, which is a non-linear approximate version of Algorithm 8. In particular, in Algorithm 9,  $f$  can be thought of as an encoder and  $g$  as a decoder. In the case where  $f(x) = Ax$ , then  $\Delta^* = g(f(\Delta)) = A^\dagger A \Delta$ . Note that by letting  $\Delta^* = \Delta/\tau$  in Algorithm 9, we recover Algorithm 6.

**Algorithm 9** REJECTION ( $p, q, X$ ) for two Gaussians with auto-encoders

**Require:**  $f, g$ ,  $p(x) = \mathcal{N}(x; m^p, \sigma^2 \text{Id})$ ,  $q(x) = \mathcal{N}(x; m^q, \sigma^2 \text{Id})$ ,  $X \sim p$ .  
 $\Delta = (m^p - m^q)/\sigma$ ,  $\Delta^* = (g(f(\Delta)))$   
 Sample  $U \sim \text{Unif}[0, 1]$ .  
 $\text{bool} = \mathbb{I}[U \leq \min(1, \exp[-\frac{1}{2}(\Delta + 2Z)^\top \Delta^*])]$   
**if**  $\text{bool}$  **then**  
     Set  $Y = X$ .  
**else**  
     Set  $Y = m^q + \sigma \left( Z - 2 \frac{Z^\top \Delta^*}{\Delta^\top \Delta^*} \Delta \right)$ .  
**end if**  
**return**  $(X, Y, \text{bool})$ .

## H. Some Theoretical Results

We consider the following setting. Let  $(\mathbf{X}_t^i)_{t \in [0,1]}$  for any  $i \in \{0, 1\}$  be given by

$$d\mathbf{X}_t^i = f_t \mathbf{X}_t^i dt + g_t d\mathbf{B}_t, \quad \mathbf{X}_0^i \sim \pi_0^i$$

where  $f : [0, 1] \rightarrow \mathbb{R}$  and  $g : [0, 1] \rightarrow [0, +\infty)$  are functions introduced further,  $\pi_0^0$  and  $\pi_0^1$  are distributions over  $\mathbb{R}^d$  and  $(\mathbf{B}_t^i)_{t \in [0,1]}$  are  $d$ -dimensional Brownian motions. In what follows, we define for any  $t \in [0, 1]$

$$f_t = -1/(1-t), \quad g_t^2 = 2t/(1-t).$$

In that case, we have that for any  $t \in [0, 1]$  and  $i \in \{0, 1\}$

$$\mathbf{X}_t^i = \alpha_t \mathbf{X}_0^i + \sigma_t \mathbf{Z}, \quad \mathbf{Z} \sim \mathcal{N}(0, \text{Id}) \tag{23}$$

with  $\alpha_t = 1-t$  and  $\sigma_t = t$ . We assume that for any  $i \in \{0, 1\}$ ,  $\pi_0^i$  has a density with respect to the Lebesgue measure denoted  $p_0^i$ . In that case, for any  $t \in [0, 1]$  and  $i \in \{0, 1\}$ ,  $\mathbf{X}_t^i$  admits a density with respect to the Lebesgue measure denoted  $p_t^i$ . In this section, we show that for any  $t \in (0, 1]$



$$\int_{\mathbb{R}^d} \|\nabla \log p_t^0(x_t) - \nabla \log p_t^1(x_t)\|^2 p_t^0(x_t) dx_t \leq C(t, p_0^0, p_0^1), \quad (24)$$

such that

1.  $\lim_{t \rightarrow 1} C(t, p_0^0, p_0^1) = 0$ ,
2.  $D(p_0^0 | p_0^1) \rightarrow 0$  implies that  $C(t, p_0^0, p_0^1) \rightarrow 0$ , where  $D$  is a measure of divergence between  $p_0^0$  and  $p_0^1$  defined further.

In other words, item 1) shows that the Fisher score between  $p_t^0$  and  $p_t^1$  gets smaller as  $t$  gets larger as expected as  $p_1^0 = p_1^1$ , a normal density. Item 2) shows that the Fisher score between  $p_t^0$  and  $p_t^1$  is small if  $p_0^0$  and  $p_0^1$  are close.

We will also establish in our main result, Theorem H.9, a lower bound for the expectation of the logarithm of the acceptance ratio in our speculative sampling setting based on (24).

**Time control.** First, we provide an upper-bound on the Fisher score that goes to 0 as  $t \rightarrow 1$ . We begin with the following result.

**Lemma H.1 (Convergence of Fisher score):** *Assume that  $\int_{\mathbb{R}^d} \|x\|^2 d\pi_0^i(x) = C_2^i < +\infty$  for  $i \in \{0, 1\}$ . Then, we have that for any  $t \in (0, 1)$  and  $i \in \{0, 1\}$*

$$\int_{\mathbb{R}^d} \|\nabla \log p_t^i(x_t) - \nabla \log p_1(x_t)\|^2 p_t^i(x_t) dx_t \leq \left(\frac{1}{\sigma_t} - \sigma_t\right)^2 d + \alpha_t^2 C_2^i,$$

where  $p_1$  is the density of  $\mathcal{N}(0, \text{Id})$  with respect to the Lebesgue measure. In addition, assume that  $\int_{\mathbb{R}^d} \|x\|^4 d\pi_0^i(x) = C_4^i < +\infty$ , we have that for any  $t \in (0, 1)$  and  $i \in \{0, 1\}$

$$\begin{aligned} \int_{\mathbb{R}^d} \|\nabla \log p_t^i(x_t) - \nabla \log p_1(x_t)\|^4 p_t^i(x_t) dx_t &\leq 3\left(\frac{1}{\sigma_t} - \sigma_t\right)^4 d^2 + \alpha_t^4 C_4^i + 6\alpha_t^2 \left(\frac{1}{\sigma_t} - \sigma_t\right)^2 C_2^i d \\ &\leq 12\left(\frac{1}{\sigma_t} - \sigma_t\right)^4 d^2 + 2\alpha_t^4 C_4^i. \end{aligned}$$

*Proof.* Let  $i \in \{0, 1\}$ . First, using Tweedie's identity, see (Vincent, 2011) for instance, we recall that for any  $t \in (0, 1)$ , we have that for any  $x_t \in \mathbb{R}^d$

$$\nabla \log p_t^i(x_t) = \int_{\mathbb{R}^d} \nabla \log p_{t|0}(x_t|x_0) p_{0|t}^i(x_0|x_t) dx_0 = \mathbb{E}[-\mathbf{Z}/\sigma_t \mid \mathbf{X}_t^i = x_t],$$

where we recall that  $\mathbf{X}_t^i = \alpha_t \mathbf{X}_0^i + \sigma_t \mathbf{Z}$ , see (23). Hence, using Jensen's inequality, we have that

$$\begin{aligned} \int_{\mathbb{R}^d} \|\nabla \log p_t^i(x_t) - \nabla \log p_1(x_t)\|^2 p_t^i(x_t) dx_t &= \mathbb{E}[\|\mathbb{E}[\mathbf{Z}/\sigma_t - \mathbf{X}_t^i \mid \mathbf{X}_t^i]\|^2] \\ &\leq \mathbb{E}[\|(\frac{1}{\sigma_t} - \sigma_t)\mathbf{Z} - \alpha_t \mathbf{X}_0^i\|^2] \\ &\leq \left(\frac{1}{\sigma_t} - \sigma_t\right)^2 \mathbb{E}[\|\mathbf{Z}\|^2] + \alpha_t^2 \mathbb{E}[\|\mathbf{X}_0^i\|^2], \end{aligned}$$

where we have used that  $\mathbf{X}_0^i$  and  $\mathbf{Z}$  are independent. Finally, using  $\mathbb{E}[\|\mathbf{Z}\|^2] = d$ , we obtained the first result. The second part of the proof is similar and left to the reader.  $\square$

We recall that for any  $\alpha \geq 1$  the  $\chi_\alpha$  divergence between two densities over  $\mathbb{R}^d$ ,  $p, q$  is given by

$$\chi_\alpha(p|q) = \int_{\mathbb{R}^d} \left(1 - \frac{p(x)}{q(x)}\right)^\alpha q(x) dx$$

If  $\alpha = 2$ , we also have

$$\chi_2(p|q) = \int_{\mathbb{R}^d} \frac{p(x)^2}{q(x)} dx - 1. \quad (25)$$

In addition, we have the following useful result.

**Lemma H.2 ( $\chi_\alpha$ -data processing inequality):** For any  $\alpha \geq 1$ ,  $t \in [0, 1]$ ,  $\chi_\alpha(p_t^0|p_t^1) \leq \chi_\alpha(p_0^0|p_0^1)$ .

Note that this data processing is in fact valid for every  $f$ -divergence with  $f$  convex. Combining Lemma H.1 and Lemma H.2, we have the following result.

**Lemma H.3 (Convergence of modified Fisher score):** Assume that  $\int_{\mathbb{R}^d} \|x\|^4 d\pi_0^i(x) = C_4^i < +\infty$  for  $i \in \{0, 1\}$ . Let  $C_4 = \max(C_4^0, C_4^1)$ . Then, we have that for any  $t \in (0, 1]$

$$\int_{\mathbb{R}^d} \|\nabla \log p_t^1(x_t) - \nabla \log p_1(x_t)\|^2 p_t^0(x_t) dx_t \leq 4(1 + \chi_2(p_0^0|p_0^1))^{1/2} \left( \left( \frac{1}{\sigma_t} - \sigma_t \right)^2 d + \alpha_t^2 C_4^{1/2} \right),$$

where  $p_1$  is the density of  $\mathcal{N}(0, \text{Id})$  with respect to the Lebesgue measure.

*Proof.* For any  $t \in (0, 1)$ , let  $A_t = \int_{\mathbb{R}^d} \|\nabla \log p_t^0(x_t) - \nabla \log p_1(x_t)\|^2 p_t^0(x_t) dx_t$ . Using the Cauchy–Schwarz inequality and (25), we have that for any  $t \in (0, 1)$

$$\begin{aligned} A_t^2 &= \left( \int_{\mathbb{R}^d} \|\nabla \log p_t^1(x_t) - \nabla \log p_1(x_t)\|^2 \frac{p_t^0(x_t)}{p_t^1(x_t)} p_t^1(x_t) dx_t \right)^2 \\ &\leq \int_{\mathbb{R}^d} \|\nabla \log p_t^1(x_t) - \nabla \log p_1(x_t)\|^4 p_t^1(x_t) dx_t \int_{\mathbb{R}^d} \frac{p_t^0(x_t)^2}{p_t^1(x_t)} dx_t \\ &\leq \int_{\mathbb{R}^d} \|\nabla \log p_t^1(x_t) - \nabla \log p_1(x_t)\|^4 p_t^1(x_t) dx_t (1 + \chi_2(p_t^0|p_t^1)). \end{aligned}$$

We conclude upon combining Lemma H.1, Lemma H.2, the fact that for any  $a, b \geq 0$ ,  $\sqrt{a+b} \leq \sqrt{a} + \sqrt{b}$  and that  $\max(\sqrt{12}, \sqrt{2}) \leq 4$ .  $\square$

Finally, combining Lemma H.3 and Lemma H.1, we get the following result.

**Proposition H.4 (Control of Fisher score (I)):** Assume that  $\int_{\mathbb{R}^d} \|x\|^4 d\pi_0^i(x) = C_4^i < +\infty$  for  $i \in \{0, 1\}$ . Let  $C_4 = \max(C_4^0, C_4^1)$ . Then, we have that for any  $t \in (0, 1]$

$$\int_{\mathbb{R}^d} \|\nabla \log p_t^0(x_t) - \nabla \log p_t^1(x_t)\|^2 p_t^0(x_t) dx_t \leq 10(1 + \chi_2(p_0^0|p_0^1))^{1/2} \left( \left( \frac{1}{\sigma_t} - \sigma_t \right)^2 d + \alpha_t^2 C_4^{1/2} \right).$$

*Proof.* For any  $t \in (0, 1)$ , we have that

$$\begin{aligned} &\int_{\mathbb{R}^d} \|\nabla \log p_t^0(x_t) - \nabla \log p_t^1(x_t)\|^2 p_t^0(x_t) dx_t \\ &\leq 2 \int_{\mathbb{R}^d} \|\nabla \log p_t^0(x_t) - \nabla \log p_1(x_t)\|^2 p_t^0(x_t) dx_t \\ &\quad + 2 \int_{\mathbb{R}^d} \|\nabla \log p_t^1(x_t) - \nabla \log p_1(x_t)\|^2 p_t^0(x_t) dx_t. \end{aligned}$$

We conclude upon combining Lemma H.1 and Lemma H.3.  $\square$

In particular, Proposition H.4 shows that  $\lim_{t \rightarrow 1} \int_{\mathbb{R}^d} \|\nabla \log p_t^0(x_t) - \nabla \log p_t^1(x_t)\|^2 p_t^0(x_t) dx_t = 0$ .

**Measure control.** We now provide a control on the Fisher score that depends on some divergence between the measures  $\pi_0^0$  and  $\pi_0^1$ . We first recall a useful result on the score which can be found in (De Bortoli et al., 2024) for instance.

**Lemma H.5 (Target Score Identity):** Assume that for any  $i \in \{0, 1\}$ ,  $p_0^i \in C^1(\mathbb{R}^d, \mathbb{R}^d)$  and for any  $t \in [0, 1]$  and  $x_t \in \mathbb{R}^d$ ,  $\int_{\mathbb{R}^d} \|\nabla \log p_0^i(x_0)\| p_{0|t}^i(x_0|x_t) dx_0 < +\infty$ . Then, we have that for any  $i \in \{0, 1\}$ ,  $t \in [0, 1]$  and  $x_t \in \mathbb{R}^d$

$$\nabla \log p_t^i(x_t) = \frac{1}{\alpha_t} \int_{\mathbb{R}^d} \nabla \log p_0^i(x_0) p_{0|t}^i(x_0|x_t) dx_0.$$

Next, we show the following result.

**Lemma H.6 (Posterior control):** We have that for any  $\alpha \geq 1$  and  $t \in (0, 1)$

$$\int_{\mathbb{R}^d} \chi_\alpha(p_{0|t}^1(x_0|x_t)|p_{0|t}^0(x_0|x_t)) p_t^0(x_t) dx_t \leq D_{0,\alpha} (\chi_{4\alpha}(p_0^1|p_0^0)^{1/4} + \chi_{4\alpha}(p_0^1|p_0^0)^{1/4}),$$

with

$$D_{0,\alpha} = 2^\alpha (1 + \chi_{2\alpha}(p_0^1|p_0^0))^{1/2} (1 + \chi_2(p_0^0|p_0^1))^{1/4}.$$

*Proof.* First, we have that for any  $\alpha \geq 1$  and  $t \in (0, 1)$

$$\begin{aligned} \int_{\mathbb{R}^d} \chi_\alpha(p_{0|t}^1(x_0|x_t)|p_{0|t}^0(x_0|x_t)) p_t^0(x_t) dx_t &= \int_{\mathbb{R}^d \times \mathbb{R}^d} \left(1 - \frac{p_{0|t}^1(x_0|x_t)}{p_{0|t}^0(x_0|x_t)}\right)^\alpha p_{0,t}^0(x_0, x_t) dx_0 dx_t \\ &= \int_{\mathbb{R}^d \times \mathbb{R}^d} \left(1 - \frac{p_0^1(x_0) p_t^0(x_t)}{p_0^0(x_0) p_t^1(x_t)}\right)^\alpha p_{0,t}^0(x_0, x_t) dx_0 dx_t \\ &\leq 2^{\alpha-1} \int_{\mathbb{R}^d} \left(1 - \frac{p_0^1(x_0)}{p_0^0(x_0)}\right)^\alpha p_0(x_0) dx_0 \\ &\quad + 2^{\alpha-1} \int_{\mathbb{R}^d \times \mathbb{R}^d} \left(\frac{p_0^1(x_0)}{p_0^0(x_0)}\right)^\alpha \left(1 - \frac{p_t^0(x_t)}{p_t^1(x_t)}\right)^\alpha p_{0,t}^0(x_0, x_t) dx_0 dx_t \\ &\leq 2^{\alpha-1} \chi_\alpha(p_0^1|p_0^0) + 2^{\alpha-1} \int_{\mathbb{R}^d \times \mathbb{R}^d} \left(\frac{p_0^1(x_0)}{p_0^0(x_0)}\right)^\alpha \left(1 - \frac{p_t^0(x_t)}{p_t^1(x_t)}\right)^\alpha p_{0,t}^0(x_0, x_t) dx_0 dx_t. \end{aligned} \quad (26)$$

Next, we note that for any  $\beta \geq 1$  and densities  $p, q$

$$\int_{\mathbb{R}^d} \left(\frac{q(x)}{p(x)}\right)^\beta p(x) dx \leq 2^{\beta-1} (1 + \chi_\beta(q|p)).$$

Using this result and (26) we have that

$$\begin{aligned} \int_{\mathbb{R}^d} \chi_\alpha(p_{0|t}^1(x_0|x_t)|p_{0|t}^0(x_0|x_t)) p_t^0(x_t) dx_t &\leq 2^{\alpha-1} \chi_\alpha(p_0^1|p_0^0) + 2^{\alpha-1} \int_{\mathbb{R}^d \times \mathbb{R}^d} \left(\frac{p_0^1(x_0)}{p_0^0(x_0)}\right)^\alpha \left(1 - \frac{p_t^0(x_t)}{p_t^1(x_t)}\right)^\alpha p_{0,t}^0(x_0, x_t) dx_0 dx_t \\ &\leq 2^{\alpha-1} \chi_\alpha(p_0^1|p_0^0) + 2^{\alpha-1} (1 + \chi_{2\alpha}(p_0^1|p_0^0))^{1/2} \left(\int_{\mathbb{R}^d} \left(1 - \frac{p_t^0(x_t)}{p_t^1(x_t)}\right)^{2\alpha} p_t^0(x_t) dx_t\right)^{1/2} \\ &\leq 2^{\alpha-1} \chi_\alpha(p_0^1|p_0^0) + 2^{\alpha-1} (1 + \chi_{2\alpha}(p_0^1|p_0^0))^{1/2} \left(\int_{\mathbb{R}^d} \left(1 - \frac{p_t^0(x_t)}{p_t^1(x_t)}\right)^{2\alpha} \frac{p_t^0(x_t)}{p_t^1(x_t)} p_t^1(x_t) dx_t\right)^{1/2} \\ &\leq 2^{\alpha-1} \chi_\alpha(p_0^1|p_0^0) + 2^{\alpha-1} (1 + \chi_{2\alpha}(p_0^1|p_0^0))^{1/2} (1 + \chi_2(p_0^0|p_0^1))^{1/4} \chi_{4\alpha}(p_t^0|p_t^1)^{1/4} \\ &\leq 2^{\alpha-1} \chi_\alpha(p_0^1|p_0^0) + 2^{\alpha-1} (1 + \chi_{2\alpha}(p_0^1|p_0^0))^{1/2} (1 + \chi_2(p_0^0|p_0^1))^{1/4} \chi_{4\alpha}(p_0^0|p_0^1)^{1/4} \\ &\leq 2^\alpha (1 + \chi_{2\alpha}(p_0^1|p_0^0))^{1/2} (1 + \chi_2(p_0^0|p_0^1))^{1/4} (\chi_{4\alpha}(p_0^0|p_0^1)^{1/4} + \chi_{4\alpha}(p_0^0|p_0^1)^{1/4}), \end{aligned}$$

which concludes the proof  $\square$

Finally, for ease of notation, we introduce for any  $t \in [0, 1]$

$$\text{FI}(p_t^0|p_t^1) = \int_{\mathbb{R}^d} \|\nabla \log p_t^0(x_t) - \nabla \log p_t^1(x_t)\|^2 p_t^0(x_t) dx_t.$$

We obtain the following result.

**Proposition H.7 (Control of Fisher score (II)):** *Assume that for any  $i \in \{0, 1\}$ ,  $p_0^i \in C^1(\mathbb{R}^d, \mathbb{R}^d)$  and for any  $t \in [0, 1]$  and  $x_t \in \mathbb{R}^d$ ,  $\int_{\mathbb{R}^d} \|\nabla \log p_0^i(x_0)\| p_{0|t}^i(x_0|x_t) dx_0 < +\infty$ . In addition, assume that for any  $i \in \{0, 1\}$ ,  $\int_{\mathbb{R}^d} \|\nabla \log p_0^i(x_0)\|^4 (p_0^0(x_0) + p_1(x_0)) dx_0 = D_4^i < +\infty$ . Then for any  $t \in [0, 1]$ , we have*

$$\int_{\mathbb{R}^d} \|\nabla \log p_t^0(x_t) - \nabla \log p_t^1(x_t)\|^2 p_t^0(x_t) dx_t \leq \frac{2D}{\alpha_t^2} (\text{FI}(p_0^0|p_0^1) + \chi_{16}(p_0^1|p_0^0)^{1/8} + \chi_{16}(p_0^0|p_0^1)^{1/8}),$$

where  $D$  is explicit in the proof.

*Proof.* For any  $t \in (0, 1)$ , let  $A_t = \int_{\mathbb{R}^d} \|\nabla \log p_t^0(x_t) - \nabla \log p_1(x_t)\|^2 p_t^0(x_t) dx_t$ . Using Lemma H.5, we have that for any  $t \in (0, 1)$

$$A_t = \frac{1}{\alpha_t^2} \int_{\mathbb{R}^d} \left\| \int_{\mathbb{R}^d} \nabla \log p_0^0(x_0) p_{0|t}^0(x_0|x_t) dx_0 - \int_{\mathbb{R}^d} \nabla \log p_0^1(x_0) p_{0|t}^1(x_0|x_t) dx_0 \right\|^2 p_t^0(x_t) dx_t.$$

Hence, for any  $t \in (0, 1)$ ,  $A_t \leq \frac{2}{\alpha_t^2} (A_t^1 + A_t^2)$  with

$$\begin{aligned} A_t^1 &= \int_{\mathbb{R}^d} \left\| \int_{\mathbb{R}^d} \nabla \log p_0^0(x_0) p_{0|t}^0(x_0|x_t) dx_0 - \int_{\mathbb{R}^d} \nabla \log p_0^1(x_0) p_{0|t}^0(x_0|x_t) dx_0 \right\|^2 p_t^0(x_t) dx_t, \\ A_t^2 &= \int_{\mathbb{R}^d} \left\| \int_{\mathbb{R}^d} \nabla \log p_0^1(x_0) p_{0|t}^0(x_0|x_t) dx_0 - \int_{\mathbb{R}^d} \nabla \log p_0^1(x_0) p_{0|t}^1(x_0|x_t) dx_0 \right\|^2 p_t^0(x_t) dx_t. \end{aligned}$$

Using Jensen's inequality, we have that for any  $t \in (0, 1)$

$$A_t^1 \leq \int_{\mathbb{R}^d} \|\nabla \log p_0^0(x_0) - \nabla \log p_0^1(x_0)\|^2 p_0^0(x_0) dx_0. \quad (27)$$

Second, using Jensen's inequality, the Cauchy–Schwarz inequality and Lemma H.6

$$\begin{aligned} A_t^2 &\leq \int_{\mathbb{R}^d \times \mathbb{R}^d} \|\nabla \log p_0^1(x_0)\|^2 \left(1 - \frac{p_{0|t}^1(x_0|x_t)}{p_{0|t}^0(x_0|x_t)}\right)^2 p_{0,t}^0(x_0, x_t) dx_0 dx_t \\ &\leq \left( \int_{\mathbb{R}^d} \|\nabla \log p_0^1(x_0)\|^4 p_0^0(x_0) dx_0 \right)^{1/2} \left( \int_{\mathbb{R}^d \times \mathbb{R}^d} \left(1 - \frac{p_{0|t}^1(x_0|x_t)}{p_{0|t}^0(x_0|x_t)}\right)^4 p_{0,t}^0(x_0, x_t) dx_0 dx_t \right)^{1/2} \\ &\leq D_{0,4}^{1/2} \left( \int_{\mathbb{R}^d} \|\nabla \log p_0^1(x_0)\|^4 p_0^0(x_0) dx_0 \right)^{1/2} (\chi_{16}(p_0^1|p_0^0)^{1/8} + \chi_{16}(p_0^0|p_0^1)^{1/8}). \end{aligned}$$

Combining this result and (27) concludes the proof with  $D = 2(1 + D_{0,4}^{1/2} \max(D_4^0, D_4^1))$ .  $\square$

Finally, combining Proposition H.4 and Proposition H.7, we get the following proposition.

**Proposition H.8 (Control Fisher (III)):** *Assume that for any  $i \in \{0, 1\}$ ,  $p_0^i \in C^1(\mathbb{R}^d, \mathbb{R}^d)$  and for any  $t \in [0, 1]$  and  $x_t \in \mathbb{R}^d$ ,  $\int_{\mathbb{R}^d} \|\nabla \log p_0^i(x_0)\| p_{0|t}^i(x_0|x_t) dx_0 < +\infty$ . In addition, assume that for any  $i \in \{0, 1\}$ ,  $\int_{\mathbb{R}^d} \|\nabla \log p_0^i(x_0)\|^4 (p_0^0(x_0) + p_1(x_0)) dx_0 = D_4^i < +\infty$ . Assume that  $\int_{\mathbb{R}^d} \|x\|^4 d\pi_0^i(x) = C_4^i < +\infty$  for  $i \in \{0, 1\}$ . Then, we have for any  $t \in (0, 1)$*

$$\begin{aligned} &\int_{\mathbb{R}^d} \|\nabla \log p_t^0(x_t) - \nabla \log p_t^1(x_t)\|^2 p_t^0(x_t) dx_t \\ &\leq C \min \left( \left(\frac{1}{\sigma_t} - \sigma_t\right)^2 + \alpha_t^2, \frac{1}{\alpha_t^2} (\text{FI}(p_0^0|p_0^1) + \chi_{16}(p_0^1|p_0^0)^{1/8} + \chi_{16}(p_0^0|p_0^1)^{1/8}) \right), \end{aligned}$$

where  $C \geq 0$  can be made explicit.

**Control of acceptance ratio.** We now provide a lower bound on the expectation of the logarithm of the acceptance ratio in the speculative sampling framework. We consider a discretization of the interval  $[0, 1]$  given by  $N \in \mathbb{N}$  and  $t_k = k/N$ . We let  $\gamma = 1/N$ . We consider the target model given for any  $k \in \{0, N-1\}$  by

$$Y_{k+1}^t = Y_k^t + \gamma \{-f_{1-t_k} Y_k^t + \frac{g_{1-t_k}^2}{2} \nabla \log p_{1-t_k}^0(Y_k)\} + \sqrt{\gamma} g_{1-t_k} Z_k^t, \quad Y_0 \sim \mathcal{N}(0, \text{Id}),$$

where  $(Z_k^t)_{k \in \mathbb{N}}$  is a sequence of i.i.d Gaussian random variables with zero mean and identity covariance matrix. We now  $k_0 \in \{0, \dots, N-1\}$ ,  $L \in \mathbb{N}$ ,  $k_L = \min(N-1, k_0 + L-1)$  and consider the draft model associated given for any  $k \in \{k_0, k_L\}$  by

$$Y_{k+1}^d = Y_k^d + \gamma \{-f_{1-t_k} Y_k^d + \frac{g_{1-t_k}^2}{2} \nabla \log p_{1-t_k}^1(Y_k)\} + \sqrt{\gamma} g_{1-t_k} Z_k^d, \quad Y_{k_0}^d = Y_{k_0}^t \sim \mathcal{N}(0, \text{Id}),$$

where  $(Z_k^d)_{k \in \mathbb{N}}$  is a sequence of i.i.d Gaussian random variables with zero mean and identity covariance matrix.

The step  $k_0 + 1$  is accepted if  $U \leq \min(1, \varphi(Z_{k_0}^t + \Delta)/\varphi(Z_{k_0}^t))$ , where  $\varphi$  is the density with respect to the Lebesgue measure of a Gaussian random variable with zero mean and identity covariance matrix and

$$\|\Delta\|^2 = \frac{\gamma g_{1-t_{k_0}}^2}{4} \|\nabla \log p_{1-t_{k_0}}^1(Y_{k_0}^t) - \nabla \log p_{1-t_{k_0}}^0(Y_{k_0}^t)\|^2.$$

Denote  $a_{k_0} = \varphi(Z_{k_0}^t + \Delta)/\varphi(Z_{k_0}^t)$ . We have that

$$\mathbb{E}[\log(a_{k_0}) \mid Y_{k_0}^t] = -\frac{1}{2} \mathbb{E}[\|\Delta\|^2 \mid Y_{k_0}^t] = -\frac{1}{2} \|\Delta\|^2.$$

Lemma 4.2 is proved in a similar way and uses  $\mathbb{E}[a_n] \geq \exp[\mathbb{E}[\log(a_n)]]$ .

**Theorem H.9 (Control of log-acceptance ratio):** Assume that for any  $i \in \{0, 1\}$ ,  $p_0^i \in C^1(\mathbb{R}^d, \mathbb{R}^d)$  and for any  $t \in [0, 1]$  and  $x_t \in \mathbb{R}^d$ ,  $\int_{\mathbb{R}^d} \|\nabla \log p_0^i(x_0)\| p_{0|t}^i(x_0|x_t) dx_0 < +\infty$ . In addition, assume that for any  $i \in \{0, 1\}$ ,  $\int_{\mathbb{R}^d} \|\nabla \log p_0^i(x_0)\|^4 (p_0^0(x_0) + p_1(x_0)) dx_0 = D_4^i < +\infty$ . Assume that  $\int_{\mathbb{R}^d} \|x\|^4 d\pi_0^i(x) = C_4^i < +\infty$  for  $i \in \{0, 1\}$ . In addition, assume that  $Y_{k_0}^t \sim p_{1-t_{k_0}}$  then

$$\begin{aligned} & \mathbb{E}[\log(a_{k_0})] \\ & \geq -C\gamma g_{s_0}^2 \min\left(\left(\frac{1}{\sigma_{s_0}} - \sigma_{s_0}\right)^2 + \alpha_{s_0}^2, \frac{1}{\alpha_{s_0}^2} (\text{FI}(p_0^0|p_0^1) + \chi_{16}(p_0^1|p_0^0)^{1/8} + \chi_{16}(p_0^0|p_0^1)^{1/8})\right), \end{aligned}$$

where  $s_0 = 1 - t_{k_0}$  and  $C \geq 0$  is explicit in the proof.

Let us interpret Theorem H.9. We aim at maximizing  $\log(a_{k_0})$  since a high acceptance ratio yields a lower computational cost of the speculative sampling method. We here give a lower bound on its expectation. There are different factors that influence this bound:

- $\gamma \rightarrow 0$  yields  $\mathbb{E}[\log(a_{k_0})] \geq 0$ . Hence a small discretization step is associated with better acceptance of the method. However, we emphasize that a small discretization step also gives a larger total number of steps. Hence the benefits of reducing the stepsize must be weighted by the additional computational requirement of having to run the speculative procedure for a larger number of iterations.
- If  $p_0^0 \rightarrow p_0^1$  (in Fisher and  $\chi_4$  divergence) then  $\mathbb{E}[\log(a_{k_0})] \geq 0$ . This means that if during speculative sampling, the two models target similar distribution then we obtain a higher acceptance rate. This remark is verified empirically in ... and echoes similar findings in LLMs (Cai et al., 2024).
- If  $g_t^2((\frac{1}{\sigma_t} - \sigma_t)^2 + \alpha_t^2) \rightarrow 0$  as  $t \rightarrow 1$  then  $\mathbb{E}[\log(a_{k_0})] \geq 0$ . Hence, in that case for low values of  $k_0$ , i.e., at the beginning of the denoising process, the acceptance rate is high. This observation is also confirmed empirically and is specific to the diffusion model setting.

In our setting, we have

$$g_t^2\left(\left(\frac{1}{\sigma_t} - \sigma_t\right)^2 + \alpha_t^2\right) = 2t(1-t)(1 + (1+1/t)^2).$$

Hence  $\lim_{t \rightarrow 1} g_t^2 \left( \left( \frac{1}{\sigma_t} - \sigma_t \right)^2 + \alpha_t^2 \right) = 0$ . Note that the proof can be trivially extended to the case where

$$Y_{k+1}^d = Y_k^d + \gamma \left\{ -f_{1-t_k} Y_k^d + \frac{(1+\varepsilon^2)g_{1-t_k}^2}{2} \nabla \log p_{1-t_k}^1(Y_k) \right\} + \sqrt{\gamma} \varepsilon g_{1-t_k} Z_k^d, \quad Y_{k_0}^d = Y_{k_0}^t \sim \mathcal{N}(0, \text{Id}).$$

In that case the *churn* parameter is no longer equal to 1 but we have  $\varepsilon \in (0, 1]$ . Finally to derive the results, we use Jensen's inequality, i.e,  $\mathbb{E}[a_n] \geq \exp[\mathbb{E}[\log(a_n)]]$ .

## I. Experimental details

In this section, we provide details about our experimental setup in Appendix I.1. Our setting for the low dimensional Gaussian Mixture Models (GMMs) is described in Appendix I.2. Similarly, our setting for the image experiments is given in Appendix I.3.

### I.1. Experiment setting.

In our setting, we consider the stochastic interpolant framework (Albergo et al., 2023) for greater flexibility. Namely, we consider a noising interpolant given by

$$\mathbf{X}_t = \alpha_t \mathbf{X}_0 + \sigma_t \mathbf{X}_1, \quad \mathbf{X}_0 \sim \pi_0, \mathbf{X}_1 \sim \mathcal{N}(0, \text{Id}), \quad (28)$$

where  $t \mapsto \alpha_t$  is a non-increasing function and  $t \mapsto \sigma_t$  is a non-decreasing function so that  $\alpha_1 = 0$ ,  $\sigma_1 = 1$ . The interpolation (28) can be associated with the following forward process

$$d\mathbf{X}_t = f_t \mathbf{X}_t dt + g_t d\mathbf{B}_t, \quad \mathbf{X}_0 \sim \pi, \quad (29)$$

where for any  $t \in (0, 1)$

$$f_t = \partial_t \log(\alpha_t), \quad g_t^2 = 2\alpha_t \sigma_t \partial_t (\sigma_t / \alpha_t).$$

The time-reversal of the noising process (29) is given by  $(\mathbf{Y}_t)_{t \in [0,1]}$  which satisfies

$$d\mathbf{Y}_t = \{-f_{1-t} \mathbf{Y}_t + g_{1-t}^2 \nabla \log p_{1-t}(\mathbf{Y}_t)\} dt + g_{1-t} d\mathbf{B}_t, \quad \mathbf{Y}_0 \sim p_1 \quad (30)$$

where  $p_t$  is the density of  $\mathbf{X}_t$  with respect to the Lebesgue measure. In practice, we do not typically know  $p_1$  and let  $\mathbf{Y}_0 \sim \mathcal{N}(0, \sigma_1^2 \text{Id})$ . For a given hyperparameter  $\varepsilon > 0$ , one can also consider

$$d\mathbf{Y}_t = \{-f_{1-t} \mathbf{Y}_t + \frac{1}{2}(1 + \varepsilon^2)g_{1-t}^2 \nabla \log p_{1-t}(\mathbf{Y}_t)\} dt + \varepsilon g_{1-t} d\mathbf{B}_t, \quad (31)$$

which has the same marginal as (30). This can also be rewritten as

$$d\mathbf{Y}_t = \{-v_{1-t}(\mathbf{Y}_t) + \frac{\varepsilon^2 g_{1-t}^2}{2} \nabla \log p_{1-t}(\mathbf{Y}_t)\} dt + \varepsilon g_{1-t} d\mathbf{B}_t, \quad (32)$$

where the so-called velocity  $v_t$  is given by

$$v_t(x) = \mathbb{E}[\partial_t \alpha_t \mathbf{X}_0 + \partial_t \sigma_t \mathbf{X}_1 \mid \mathbf{X}_t = x].$$

Upon combining (31) and (32), we have that for any  $t \in (0, 1)$

$$\nabla \log p_t(x) = -\mathbb{E}[\mathbf{X}_1 \mid \mathbf{X}_t = x] / \sigma_t = \frac{2}{g_t^2} (f_t x - v_t(x)). \quad (33)$$

In particular, in order to estimate the score function, we only need to estimate the velocity and vice-versa. In practice, we consider the following loss function

$$\mathcal{L}_\theta = \int_0^1 \mathbb{E}[\|\partial_t \alpha_t \mathbf{X}_0 + \partial_t \sigma_t \mathbf{X}_1 - v_{\theta,t}(\mathbf{X}_t)\|^2] w_t dt,$$

where  $w_t$  is a weighting term, see Esser et al. (2024) for some possible choices for  $w_t$ . We denote  $s_\theta$  the score estimated from  $v_\theta$  using (33). At sampling time, we consider the Euler–Maruyama discretisation of (32). More precisely, we define some timesteps  $\{t_i\}_{i=0}^N$  with  $0 = t_0 < t_1 < \dots < t_N = 1$  and consider the following Markov chain

$$Y_{k+1} = Y_k + \gamma_k \left\{ v_{\theta, 1-t_k}(Y_k) + \frac{\varepsilon^2 g_{1-t_k}^2}{2} s_{\theta, 1-t_k}(Y_k) \right\} + \sqrt{\gamma_k} \varepsilon g_{1-t_k} Z_k, \quad (34)$$



where  $(Z_k)_{k \in \mathbb{N}}$  is a sequence of independent and identically distributed Gaussian random variables with zero mean and identity covariance matrix and  $\gamma_k = t_{k+1} - t_k$ . Note that in practice, in the case where additional conditioning information is available, one can consider an additional guidance term and (34) is changed into

$$Y_{k+1} = Y_k + \gamma_k \left\{ (1 + \delta) v_{\theta, 1-t_k}(Y_k, c) - \delta v_{\theta, 1-t_k}(Y_k, \emptyset) + \frac{\varepsilon^2 g_{1-t_k}^2}{2} s_{\theta, 1-t_k}(Y_k) \right\} + \sqrt{\gamma_k} \varepsilon g_{1-t_k} Z_k,$$

where  $v_{\theta, t}(\cdot, c)$  corresponds to a *conditional* model and  $v_{\theta, t}(\cdot, \emptyset)$  to an unconditional one.

## I.2. Low dimensional experiments.

In our low dimensional setting, we create a dataset by sampling from a mixture of Gaussians distribution with means uniformly and independently sampled in  $[-2, 2]^d$  where  $d$  is the dimension. For each Gaussian component, we consider a covariance matrix of the form  $\sigma^2 \text{Id}$ , where  $\sigma > 0$  is the standard deviation. The standard deviation of each Gaussian component is also random, uniformly and independently distributed on  $[0.1, 0.2]$ . We sweep over the dimension  $d \in \{2, 4, 8, 16, 32\}$  and the number of components  $n \in \{1, 2, 4, 8, 16\}$ . The velocity of the diffusion model is parameterised with a sequence of MLPs. For all MLP we use the GeLU activation function. The label, corresponding to the component of the mixture is encoded using a layer embedding layer with feature dimension 512. Similarly, the time information is encoded using sinusoidal embedding with feature dimension 512. This encoding is then processed with a MLP with output dimension 512. The time embedding and the label embedding are then concatenated into a conditioning embedding. The conditioning embedding and the input  $x_t$  of the velocity network are then processed independently with 3 MLP layers with output dimension (64, 64, 128). The obtained embedding are then concatenated and processed with 3 MLP layers with output dimension (128, 64, 64). Finally a last dense layer with output dimension  $d$  is added. We do not consider any normalisation layer. In the case of the training of an independent draft model, the three preprocessing MLP layers are replaced with one MLP layer with output dimension 4. Similarly, the three postprocessing MLP layers are replaced with one MLP layer with output dimension 4. For the sampling, we use 250 sampling steps. We refer to Appendix J for additional results.

## I.3. Image experiments

All FID and IS scores are evaluated with  $50k$  images.

**CIFAR10.** The shape of the samples in the training dataset is  $(32 \times 32 \times 3)$ . The batch size is set to 128. Images are rescaled between  $-1.0$  and  $1.0$ . We consider an augmentation pipeline similar to the one of (Karras et al., 2022). The augmentation pipeline is applied with a global probability  $p = 0.12$ . The rest of the augmentation pipeline is similar to the one used in (Karras et al., 2022). In particular, we consider flipping (both  $x$  and  $y$  axis), anisotropy transformations, non-integer rotation, scaling and non-integer translation.

For the model, we consider a  $U$ -net architecture with GeLU activations, 4 levels with a residual attention block applied on the second level. The channel multipliers are given by  $(1, 2, 2, 2)$ . The channel size is 256. We consider a dropout rate of 0.2. The normalization layers are RMS normalization layers. For the attention layers we consider 8 heads. The number of residual blocks is 2. For the skip connection, we add (and normalize) the current activation with the stored activation. The time is embedded using sinusoidal embedding with hidden dimension 256. We embed the 10 different classes and consider conditional models. We also condition the model on the augmentation vector. These two conditionings are added and the time embedding is added on top of this. The conditioning occurs through adaptive normalization layers. We train the model for  $1M$  steps with the Adam optimizer and a learning rate of  $10^{-4}$  and EMA decay of 0.9999.

**LSUN.** We consider the same configuration as CIFAR10. However, the samples do not have label and we only consider the augmentation conditioning.

## I.4. Latent CIFAR-10 experiments

In the first stage, as an auto-encoder, we use variational auto-encoder (VAE) (Kingma & Welling, 2014) with a smaller term  $\beta$  on the KL-term as in  $\beta$ -VAE (Higgins et al., 2016). The encoder and decoder are represented by U-Net where in encoder, U-Net follows only the downsampling and middle bottleneck paths, while in decoder, U-Net follows middle bottleneck and upsampling paths, which is similar to what is used in (Rombach et al., 2022). We use 128 channels for the corresponding U-Nets without attention in downsampling/upsampling but with attention in the middle (1 head) and with channel multipliers

(1, 2, 4, 4). We use SILU activation function. We also use RMSNorm as normalization as opposed to GroupNorm. We also employ perceptual LPSIS loss (Zhang et al., 2018) with coefficient 1 as well as patch-based discriminator as in (Esser et al., 2021). The dimensionality of the latent space is (4, 4, 32) which is 6 times smaller than the original CIFAR-10 image dimensionality (32, 32, 3). We train the autoencoder for 500000 steps. We track the FID on the subset of 12800 images comparing clean images and the reconstructions  $\text{decoder}(\text{encoder}(x))$ , and select hyperparameters which achieve the smallest FID. The selected hyperparameters as well as their ranges are:

- Number of discriminator filters = 32. Range [32, 64, 128].
- Number of discriminator layers = 6. Range [3, 6, 9].
- Dropout rate for both encoder and decoder = 0.0. Range [0, 0.1, 0.2, 0.3].
- $\beta$  parameter =  $1e - 6$ . Range [ $1e - 4$ ,  $5e - 5$ ,  $1e - 5$ ,  $5e - 6$ ,  $1e - 6$ ,  $5e - 7$ ,  $1e - 7$ ].
- Generator loss coefficient = 0.01. Range [0.001, 0.01, 0.1, 1.0].
- Adversarial loss coefficient = 0.001. Range [0.001, 0.01, 0.1, 1.0].
- Batch size = 1024. Range [128, 256, 512, 1024]

For the second stage, we freeze the encoder and decoder and train a diffusion model on the encoded images (we take the means), similar to (Rombach et al., 2022). We use the U-Net with 256 channels, (2, 2) channel multipliers with attention performed (False, True), with attention in the middle with 8 attention heads, RMSNorm, GeLU activation. We train latent diffusion for 160000 iterations with batch size 256. We track FID on the subset of 12800 to select the hyperparameters. The selected hyperparameters as well as their ranges are:

- Prediction target =  $x_0$ . Range  $x_0$  or velocity
- U-Net dropout rate = 0.0. Range [0, 0.1, 0.2, 0.3].
- Learning rate =  $1e - 4$ . Range [ $1e - 3$ ,  $1e - 4$ ,  $5e - 5$ ]
- Noise process type = cosine. Range - linear, cosine, rectified flow

Once the models are trained, we employ the same sampling strategy as in CIFAR-10 experiment.

### I.5. PushT dataset.

We consider the PushT dataset. The task here is to push a  $T$  shape onto a target shape on a two dimensional plane. The action dimension is 2, the action horizon is 8. We keep an history of length 2 and consider a maximum of 300 steps when unrolling the policy. We consider a prediction horizon of length 16. This means that the dimension of the target is  $16 \times 2$ . And we condition on the last two previous states (dimension is 5). Hence the conditioning signal has shape  $(2 \times 5)$ . Once we have predicted 16 actions we execute 8 of them. As specified before we execute a maximum of 300 steps or stop if the reward reaches one, i.e., the  $T$  shape is perfectly aligned.

We train the model for  $1M$  steps with Adam and stepsize  $10^{-4}$ . We consider a one-dimensional U-net with time embedding. The architecture follows from (Chi et al., 2023).

At inference time, we rely on the DDPM sampler.

## J. Additional results

We run similar experiments in latent space to showcase the flexibility of our method. We follow the approach described in (Rombach et al., 2022) – we pre-train an autoencoder on the whole dataset and then train a diffusion model on the latent-encoded dataset. We consider the latent space of shape  $(4 \times 4 \times 32)$  which is 6 times smaller than the dimensionality  $(32 \times 32 \times 3)$  of CIFAR10. We refer to Appendix I.4 for architectural and training details. We report FID score computed on 50k training samples. Our results are reported in Table 3. We found that using latent diffusion on CIFAR-10 achieved better

## Accelerated Diffusion Models via Speculative Sampling

Configuration	Draft		Target (30 steps)		Target (10 steps)		Speculative		
	FID ↓	IS ↑	FID ↓	IS ↑	FID ↓	IS ↑	FID ↓	IS ↑	NFE ↓
$\epsilon = 0.01, \tau = 0.5$	<b>80.92</b>	<b>5.59</b>	2.67	11.09	<b>39.48</b>	<b>7.42</b>	2.66	11.13	18.53
$\epsilon = 0.01, \tau = 1.0$	<b>80.92</b>	<b>5.59</b>	2.67	11.09	<b>39.48</b>	<b>7.42</b>	2.66	11.14	17.78
$\epsilon = 0.01, \tau = 2.0$	<b>80.92</b>	<b>5.59</b>	2.67	11.09	<b>39.48</b>	<b>7.42</b>	2.66	11.14	17.09
$\epsilon = 0.25, \tau = 0.5$	82.28	5.50	2.64	<b>11.15</b>	87.39	4.82	2.68	11.18	10.37
$\epsilon = 0.25, \tau = 1.0$	82.28	5.50	2.64	<b>11.15</b>	87.39	4.82	2.66	<b>11.23</b>	9.36
$\epsilon = 0.25, \tau = 2.0$	82.28	5.50	2.64	<b>11.15</b>	87.39	4.82	2.66	11.21	8.36
$\epsilon = 0.5, \tau = 0.5$	83.27	5.42	<b>2.51</b>	11.08	118.78	3.81	2.56	11.11	9.35
$\epsilon = 0.5, \tau = 1.0$	83.27	5.42	<b>2.51</b>	11.08	118.78	3.81	<b>2.50</b>	11.12	8.30
$\epsilon = 0.5, \tau = 2.0$	83.27	5.42	<b>2.51</b>	11.08	118.78	3.81	2.52	11.07	7.30
$\epsilon = 1.0, \tau = 0.5$	97.67	4.72	37.54	7.09	182.94	2.43	37.13	7.11	9.57
$\epsilon = 1.0, \tau = 1.0$	97.67	4.72	37.54	7.09	182.94	2.43	37.85	7.07	8.36
$\epsilon = 1.0, \tau = 2.0$	97.67	4.72	37.54	7.09	182.94	2.43	38.32	7.09	<b>7.19</b>

Table 3. Latent diffusion on CIFAR-10 with window size = 15 for speculative sampling. For each column, we report the best result in **bold**.

Configuration	Draft		Target (500 steps)		Speculative		
	FID ↓	IS ↑	FID ↓	IS ↑	FID ↓	IS ↑	NFE ↓
$\epsilon = 0.005, \tau = 0.25$	<b>5.76</b>	1.93	4.66	<b>2.02</b>	4.69	2.01	305.39
$\epsilon = 0.005, \tau = 0.5$	<b>5.76</b>	1.93	4.66	<b>2.02</b>	4.68	2.01	286.07
$\epsilon = 0.005, \tau = 1.0$	<b>5.76</b>	1.93	4.66	<b>2.02</b>	4.70	2.01	263.56
$\epsilon = 0.005, \tau = 2.0$	<b>5.76</b>	1.93	4.66	<b>2.02</b>	4.72	2.01	238.01
$\epsilon = 0.01, \tau = 0.25$	<b>5.76</b>	1.93	4.66	<b>2.02</b>	4.65	2.01	257.96
$\epsilon = 0.01, \tau = 0.5$	<b>5.76</b>	1.93	4.66	<b>2.02</b>	4.67	2.01	236.04
$\epsilon = 0.01, \tau = 1.0$	<b>5.76</b>	1.93	4.66	<b>2.02</b>	4.69	2.00	211.47
$\epsilon = 0.01, \tau = 2.0$	<b>5.76</b>	1.93	4.66	<b>2.02</b>	4.76	2.00	184.98
$\epsilon = 0.05, \tau = 0.25$	5.97	1.91	4.66	2.01	4.48	2.02	186.63
$\epsilon = 0.05, \tau = 0.5$	5.97	1.91	4.66	2.01	4.53	2.00	164.07
$\epsilon = 0.05, \tau = 1.0$	5.97	1.91	4.66	2.01	4.62	2.01	140.06
$\epsilon = 0.05, \tau = 2.0$	5.97	1.91	4.66	2.01	4.86	1.99	116.38
$\epsilon = 0.1, \tau = 0.25$	6.46	1.91	4.52	2.00	4.36	<b>2.03</b>	176.02
$\epsilon = 0.1, \tau = 0.5$	6.46	1.91	4.52	2.00	4.38	2.02	154.73
$\epsilon = 0.1, \tau = 1.0$	6.46	1.91	4.52	2.00	4.56	1.99	131.47
$\epsilon = 0.1, \tau = 2.0$	6.46	1.91	4.52	2.00	4.79	1.97	108.40
$\epsilon = 0.25, \tau = 0.25$	10.11	1.96	<b>4.13</b>	1.96	3.94	2.01	172.65
$\epsilon = 0.25, \tau = 0.5$	10.11	1.96	<b>4.13</b>	1.96	3.98	1.97	153.05
$\epsilon = 0.25, \tau = 1.0$	10.11	1.96	<b>4.13</b>	1.96	4.24	1.97	130.71
$\epsilon = 0.25, \tau = 2.0$	10.11	1.96	<b>4.13</b>	1.96	4.53	1.96	<b>107.92</b>
$\epsilon = 0.5, \tau = 0.25$	17.53	<b>2.11</b>	4.18	1.96	<b>4.02</b>	1.96	178.45
$\epsilon = 0.5, \tau = 0.5$	17.53	<b>2.11</b>	4.18	1.96	<b>4.02</b>	1.95	160.68
$\epsilon = 0.5, \tau = 1.0$	17.53	<b>2.11</b>	4.18	1.96	4.26	1.93	139.16
$\epsilon = 0.5, \tau = 2.0$	17.53	<b>2.11</b>	4.18	1.96	4.51	1.93	116.33

Table 4. LSUN with window size = 50, no last step function, 500 steps. For each column, we report the best result in **bold**.

FID score when the target used only 30 sampling iterations. Nevertheless, we see that our speculative sampling method still provides 3-x speed-up (best is NFE) while maintaining similar to target model quality. We also considered using target model with only 10 NFEs and Table 3 suggests that it achieves considerably worse results. This highlights the strength of our approach.

Accelerated Diffusion Models via Speculative Sampling

Configuration	Draft		Target (200 steps)		Speculative		
	FID ↓	IS ↑	FID ↓	IS ↑	FID ↓	IS ↑	NFE ↓
$\epsilon = 0.001, \tau = 0.25$	<b>10.56</b>	1.89	3.99	<b>1.99</b>	3.99	1.98	176.85
$\epsilon = 0.001, \tau = 0.5$	<b>10.56</b>	1.89	3.99	<b>1.99</b>	3.99	1.98	173.49
$\epsilon = 0.001, \tau = 1.0$	<b>10.56</b>	1.89	3.99	<b>1.99</b>	3.99	1.98	168.23
$\epsilon = 0.001, \tau = 2.0$	<b>10.56</b>	1.89	3.99	<b>1.99</b>	3.99	1.98	160.89
$\epsilon = 0.005, \tau = 0.25$	10.58	1.89	4.02	1.98	4.00	1.98	137.95
$\epsilon = 0.005, \tau = 0.5$	10.58	1.89	4.02	1.98	3.99	1.98	131.53
$\epsilon = 0.005, \tau = 1.0$	10.58	1.89	4.02	1.98	3.99	1.98	124.52
$\epsilon = 0.005, \tau = 2.0$	10.58	1.89	4.02	1.98	4.00	1.98	117.13
$\epsilon = 0.01, \tau = 0.25$	10.63	1.89	3.99	1.98	3.98	1.98	121.26
$\epsilon = 0.01, \tau = 0.5$	10.63	1.89	3.99	1.98	3.98	1.98	114.51
$\epsilon = 0.01, \tau = 1.0$	10.63	1.89	3.99	1.98	3.99	1.98	107.26
$\epsilon = 0.01, \tau = 2.0$	10.63	1.89	3.99	1.98	4.01	1.98	99.20
$\epsilon = 0.05, \tau = 0.25$	12.73	1.91	3.95	1.98	3.94	1.98	92.66
$\epsilon = 0.05, \tau = 0.5$	12.73	1.91	3.95	1.98	3.96	1.97	86.26
$\epsilon = 0.05, \tau = 1.0$	12.73	1.91	3.95	1.98	4.03	1.96	78.75
$\epsilon = 0.05, \tau = 2.0$	12.73	1.91	3.95	1.98	4.14	1.95	70.04
$\epsilon = 0.1, \tau = 0.25$	18.56	1.99	3.92	1.99	3.89	1.97	87.74
$\epsilon = 0.1, \tau = 0.5$	18.56	1.99	3.92	1.99	3.93	<b>1.99</b>	82.05
$\epsilon = 0.1, \tau = 1.0$	18.56	1.99	3.92	1.99	3.97	1.98	74.87
$\epsilon = 0.1, \tau = 2.0$	18.56	1.99	3.92	1.99	4.16	1.94	66.28
$\epsilon = 0.25, \tau = 0.25$	33.76	2.28	<b>3.83</b>	1.94	3.76	1.96	85.60
$\epsilon = 0.25, \tau = 0.5$	33.76	2.28	<b>3.83</b>	1.94	<b>3.74</b>	1.97	80.82
$\epsilon = 0.25, \tau = 1.0$	33.76	2.28	<b>3.83</b>	1.94	3.94	1.95	74.27
$\epsilon = 0.25, \tau = 2.0$	33.76	2.28	<b>3.83</b>	1.94	4.12	1.94	<b>66.01</b>
$\epsilon = 0.5, \tau = 0.25$	49.82	2.65	4.09	1.95	3.93	1.95	87.12
$\epsilon = 0.5, \tau = 0.5$	49.82	2.65	4.09	1.95	3.97	1.95	83.29
$\epsilon = 0.5, \tau = 1.0$	49.82	2.65	4.09	1.95	4.14	1.93	77.55
$\epsilon = 0.5, \tau = 2.0$	49.82	2.65	4.09	1.95	4.22	1.96	69.81
$\epsilon = 1.0, \tau = 0.25$	115.98	<b>3.44</b>	4.76	1.93	4.75	1.95	93.13
$\epsilon = 1.0, \tau = 0.5$	115.98	<b>3.44</b>	4.76	1.93	4.73	1.97	90.88
$\epsilon = 1.0, \tau = 1.0$	115.98	<b>3.44</b>	4.76	1.93	4.77	1.96	87.24
$\epsilon = 1.0, \tau = 2.0$	115.98	<b>3.44</b>	4.76	1.93	4.85	1.95	81.40

Table 5. LSUN with window size = 50, no last step function, 200 steps. For each column, we report the best result in **bold**.

Configuration	Draft		Target (100 steps)		Speculative		
	FID ↓	IS ↑	FID ↓	IS ↑	FID ↓	IS ↑	NFE ↓
$\epsilon = 0.001, \tau = 0.25$	<b>24.04</b>	1.99	3.81	1.95	3.78	1.95	91.82
$\epsilon = 0.001, \tau = 0.5$	<b>24.04</b>	1.99	3.81	1.95	3.79	1.95	90.57
$\epsilon = 0.001, \tau = 1.0$	<b>24.04</b>	1.99	3.81	1.95	3.79	1.95	88.56
$\epsilon = 0.001, \tau = 2.0$	<b>24.04</b>	1.99	3.81	1.95	3.79	1.95	85.46
$\epsilon = 0.005, \tau = 0.25$	24.26	2.00	3.81	1.95	3.78	1.95	73.13
$\epsilon = 0.005, \tau = 0.5$	24.26	2.00	3.81	1.95	3.77	1.95	70.13
$\epsilon = 0.005, \tau = 1.0$	24.26	2.00	3.81	1.95	3.77	1.95	66.67
$\epsilon = 0.005, \tau = 2.0$	24.26	2.00	3.81	1.95	3.77	1.95	63.10
$\epsilon = 0.01, \tau = 0.25$	25.05	2.01	3.80	1.95	3.77	1.94	65.75
$\epsilon = 0.01, \tau = 0.5$	25.05	2.01	3.80	1.95	3.77	1.94	62.68
$\epsilon = 0.01, \tau = 1.0$	25.05	2.01	3.80	1.95	3.77	1.94	59.59
$\epsilon = 0.01, \tau = 2.0$	25.05	2.01	3.80	1.95	3.77	1.94	56.71
$\epsilon = 0.05, \tau = 0.25$	48.62	2.27	3.75	1.96	<b>3.75</b>	1.94	52.44
$\epsilon = 0.05, \tau = 0.5$	48.62	2.27	3.75	1.96	3.76	1.93	50.07
$\epsilon = 0.05, \tau = 1.0$	48.62	2.27	3.75	1.96	3.77	1.93	47.57
$\epsilon = 0.05, \tau = 2.0$	48.62	2.27	3.75	1.96	3.85	1.93	44.52
$\epsilon = 0.1, \tau = 0.25$	69.55	2.53	<b>3.74</b>	1.95	3.78	1.94	49.65
$\epsilon = 0.1, \tau = 0.5$	69.55	2.53	<b>3.74</b>	1.95	3.79	1.94	47.75
$\epsilon = 0.1, \tau = 1.0$	69.55	2.53	<b>3.74</b>	1.95	3.79	1.93	45.51
$\epsilon = 0.1, \tau = 2.0$	69.55	2.53	<b>3.74</b>	1.95	3.86	1.91	42.52
$\epsilon = 0.25, \tau = 0.25$	97.47	3.17	3.85	1.92	3.79	1.93	48.11
$\epsilon = 0.25, \tau = 0.5$	97.47	3.17	3.85	1.92	3.82	1.94	46.76
$\epsilon = 0.25, \tau = 1.0$	97.47	3.17	3.85	1.92	3.81	1.93	44.92
$\epsilon = 0.25, \tau = 2.0$	97.47	3.17	3.85	1.92	3.90	1.92	<b>42.16</b>
$\epsilon = 0.5, \tau = 0.25$	147.36	<b>3.62</b>	4.08	1.97	4.01	1.95	48.38
$\epsilon = 0.5, \tau = 0.5$	147.36	<b>3.62</b>	4.08	1.97	4.06	1.96	47.43
$\epsilon = 0.5, \tau = 1.0$	147.36	<b>3.62</b>	4.08	1.97	4.14	1.95	46.02
$\epsilon = 0.5, \tau = 2.0$	147.36	<b>3.62</b>	4.08	1.97	4.21	1.95	43.70
$\epsilon = 1.0, \tau = 0.25$	231.66	2.74	5.76	<b>2.02</b>	5.72	2.00	50.08
$\epsilon = 1.0, \tau = 0.5$	231.66	2.74	5.76	<b>2.02</b>	5.69	2.00	49.59
$\epsilon = 1.0, \tau = 1.0$	231.66	2.74	5.76	<b>2.02</b>	5.70	2.01	49.00
$\epsilon = 1.0, \tau = 2.0$	231.66	2.74	5.76	<b>2.02</b>	5.65	<b>2.02</b>	47.89

Table 6. LSUN with window size = 50, no last functions, 100 steps. For each column, we report the best result in **bold**.